

Role and Structure of the Magnetic Field in Extragalactic Jets

Lukasz Stawarz & Roger Blandford

Stanford University

Outline of the Talk

- Introduction
- Jet Launching (extraction of the energy and angular momentum from the black hole/accretion disk system)
- Jet Formation (collimation and acceleration of the nuclear outflow)
- Jet Propagation (confinement, stability, and morphology of magnetized jets)
- Jet Emission (particle acceleration and radiative properties)
- Summary

Jets: Magnetized Fluids

Magnetic field (MF) assures fluid-like character of the jet plasma and is a source of a fluid viscosity*.

$$\langle v_e \rangle \approx \left(\frac{kT}{m_e} \right)^{1/2} \quad \text{mean velocity of thermal electrons}$$

$$\lambda_C = \frac{\langle v_e \rangle}{\omega_{\text{col}}^{ee}} \quad \text{where} \quad \omega_{\text{col}}^{ee} = \frac{2\pi e^4 n_{\text{pl}} \ln \Lambda}{m_e^2 (3kT/m_e)^{3/2}} \approx \sqrt{\frac{m_p}{m_e}} \omega_{\text{col}}^{pp} \approx \frac{m_p}{m_e} \omega_{\text{col}}^{ep} \quad \text{Coulomb mean free path}$$

$$r_L = \frac{\langle v_e \rangle}{\omega_L^e} \quad \text{where} \quad \omega_L^e = \frac{eB}{m_e c} \quad \text{electron gyroradius}$$

$$\lambda_D = \frac{\langle v_e \rangle}{\omega_{\text{pl}}^e} \quad \text{where} \quad \omega_{\text{pl}}^e = \left(\frac{4\pi e^2 n_{\text{pl}}}{m_e} \right)^{1/2} \quad \text{Debye screening length}$$

$$\lambda_C \gg \ell \gg \lambda_D, r_L \quad \text{jets: collisionless neutral plasma}$$

(* conventional viscosity based on Coulomb scattering is irrelevant; Baan 80, Begelman 82, Kahn 83)

For Illustration: NR MHD

$$\vec{\nabla} \times \vec{B} = \frac{4\pi}{c} \vec{j} + \frac{1}{c} \frac{\partial}{\partial t} \vec{E} \quad (\text{Amper})$$

$$\vec{\nabla} \times \vec{E} = -\frac{1}{c} \frac{\partial}{\partial t} \vec{B} \quad (\text{Faraday})$$

$$\vec{\nabla} \cdot \vec{B} = 0 \quad (\text{Gauss})$$

$$\vec{\nabla} \cdot \vec{E} = 4\pi Q \quad (\text{Poisson})$$

Order-of-magnitude analysis indicates

$$E \sim (v/c) B$$

$$c Q \sim (v/c) j$$

Thus, in a non-relativistic regime $v \ll c$

one can neglect the convective and displacement currents, as well as all the electric forces acting on plasma particles.

Non-relativistic Ohm's law
(assuming plasma resistivity η is a scalar)

although it is not...

$$\eta \vec{j} = \vec{E} + \vec{\beta} \times \vec{B}$$

Induction equation
(advection and diffusion of MF)

$$\frac{\partial}{\partial t} \vec{B} = \vec{\nabla} \times (\vec{v} \times \vec{B}) + D_M (\vec{\nabla}^2 \vec{B})$$

Magnetic diffusivity and
magnetic Reynolds number

$$D_M = \frac{c^2 \eta}{4\pi}, \quad \mathcal{R}_M = \frac{t_{\text{diff}}}{t_{\text{adv}}} = \frac{\ell v}{D_M}$$

Lorentz force
(tension and gradient pressure of MF)

$$\frac{1}{c} \vec{j} \times \vec{B} = \frac{1}{4\pi} (\vec{\nabla} \times \vec{B}) \times \vec{B}$$

Further Approximations

$$\frac{\partial}{\partial t} \vec{B} = \vec{\nabla} \times (\vec{v} \times \vec{B})$$

$$\frac{\partial}{\partial t} \rho + \vec{\nabla} \cdot (\rho \vec{v}) = 0$$

$$\left(\frac{\partial}{\partial t} + \vec{v} \cdot \vec{\nabla} \right) \left(\frac{p}{\rho^{\hat{\gamma}}} \right) = 0$$

$$\rho \left(\frac{\partial}{\partial t} + \vec{v} \cdot \vec{\nabla} \right) \vec{v} = -\vec{\nabla} p + \frac{1}{4\pi} \left(\vec{\nabla} \times \vec{B} \right) \times \vec{B}$$

Ideal MHD:
perfect conductivity limit

$$\eta \rightarrow 0 \quad (\text{or } R_M \gg 1)$$

Electric field (EF) vanishes in the plasma rest frame. MF is advected with the plasma so that the magnetic flux is conserved ('flux freezing').

Non-relativistic Force-Free:

$$\beta_M \ll 1 \quad \text{and} \quad \sigma \gg 1$$

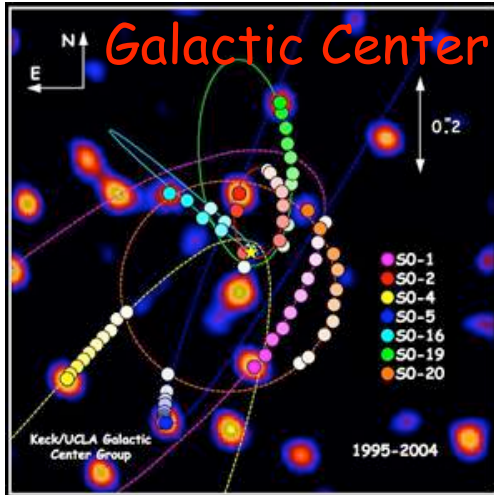
MF is in equilibrium with itself (balance between MF pressure and tension forces).
Currents flow parallel to the field lines.

$$\sigma \equiv \frac{v_A^2}{v^2} = \frac{U_B}{U_{\text{kin}}} = \frac{B^2}{4\pi\rho v^2}$$

$$\beta_M \equiv \frac{p}{U_B} = \frac{8\pi p}{B^2}$$

$$\vec{j} \times \vec{B} = 0$$

Supermassive Black Holes



“No Hair” theorem: BH is characterized solely by its mass M and angular momentum J (Kerr 63; no electric charge assumed), no matter on the history of the formation process. Thus, BH cannot have its own MF. However, BH can be merged into an external MF supported by external currents. The maximum energy density of such field (B_E) is therefore equal to the energy density of the matter accreting at the Eddington rate (L_E).
 [e.g., Rees 84, Begelman 02 and ref. therein]

$$r_g = \frac{GM}{c^2} \approx 10^{13} M_8 [\text{cm}] \quad \text{where} \quad M_8 \equiv \frac{M}{10^8 M_\odot}$$

$$a = \frac{J}{Mc} \quad \text{and} \quad a_{\text{max}} = r_g$$

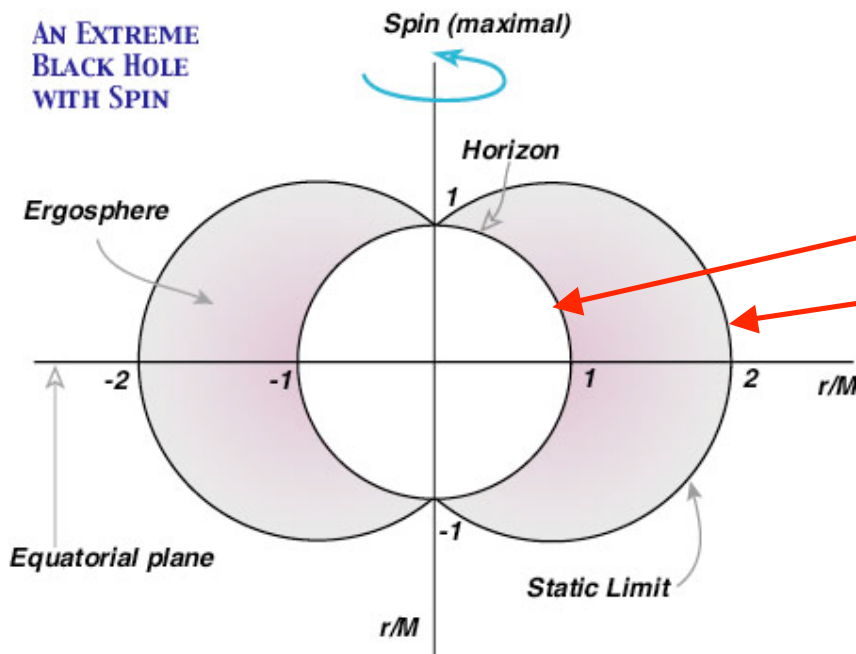
$$r_S = r_g + \sqrt{r_g^2 - a^2}, \quad r_C = r_g + \sqrt{r_g^2 - a^2 \cos^2 \theta}$$

$$\Omega_S = \left(\frac{J}{J_{\text{max}}} \right) \frac{c}{2r_S}$$

$$L_E = \frac{4\pi GMm_p c}{\sigma_T} \approx 10^{46} M_8 [\text{erg/s}]$$

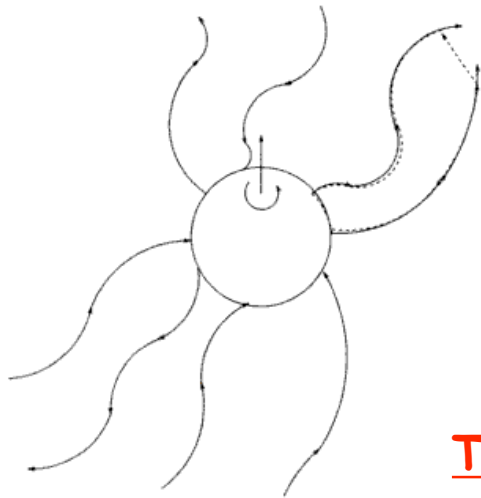
$$B_E = \left(\frac{2L_E}{r_g^2 c} \right)^{1/2} \approx 6 \times 10^4 M_8^{-1/2} [\text{G}].$$

AN EXTREME BLACK HOLE WITH SPIN



How Much Power Is Available?

BH embedded in a uniform MF acquires a quadrupole distribution of the electric charges with the corresponding poloidal electric field (Wald 74, Phinney 83). Thus, power can be extracted by allowing currents to flow between the equator and poles of a spinning BH within the magnetosphere above the event horizon (“unipolar inductor”). For the conserved magnetic flux and $\mathbf{B} \sim \mathbf{B}_E$, the Faraday and Gauss laws imply the potential drop (electromotive force) involved



$$\Delta V \equiv - \oint \vec{E} \cdot d\vec{l} = \oint \left(\frac{\vec{v}}{c} \times \vec{B} \right) \cdot d\vec{l} \sim \frac{J B r_g}{J_{\max}} \sim 10^{18} M_8^{1/2} \frac{J}{J_{\max}} \text{ [cgs]}$$

$$E_{\max} \sim e \Delta V \sim 3 \times 10^{20} M_8^{1/2} \frac{J}{J_{\max}} \text{ [eV]} \quad \text{UHECRs!}$$

(emf results from different velocities of ZAMOs at different distances from BH)

This gives the maximum power that can be extracted:

$$P \sim \Delta V \cdot I \sim \frac{\Delta V^2}{\mathfrak{R}} \sim \frac{c}{4\pi} \left(\frac{J}{J_{\max}} \right)^2 B^2 r_g^2 \sim 10^{45} M_8 \left(\frac{J}{J_{\max}} \right)^2 \text{ [erg/s]}$$

(The event horizon of BH behaves like a spinning conductor with finite conductivity. Hence $D_M \sim r_g c$, since MF has to decay just like its supporting currents flowing into the event horizon on the dynamical timescale $\sim r_g/c$. This gives the BH resistance $\mathfrak{R} \sim 4\pi/c$.)

How To Extract This Power?

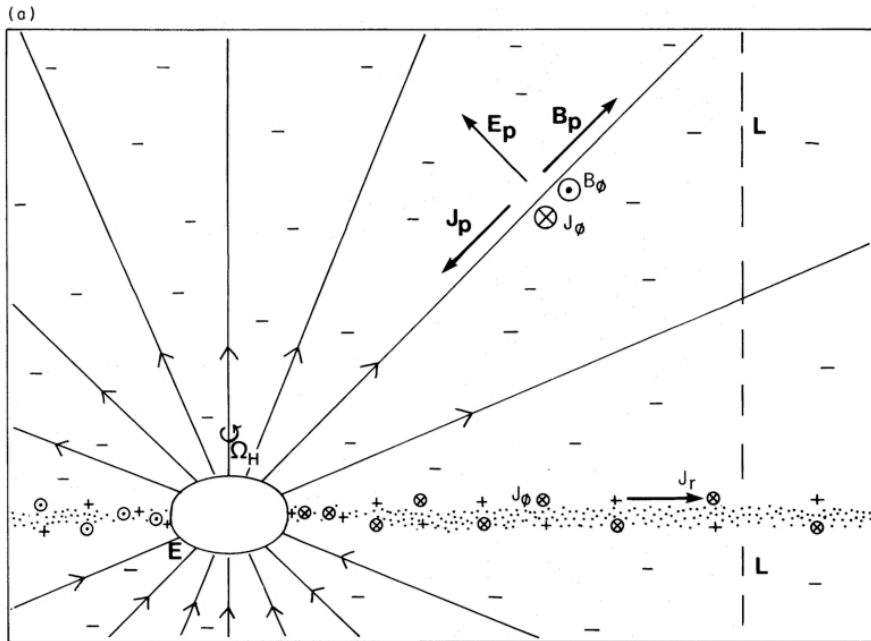
Blandford & Znajek 77: with a force-free magnetosphere added to a rotating BH embedded in an external MF, electromagnetic currents are driven, and the energy is released in the expense of the BH rotational energy ("reducible mass")

$$E_{\text{rot}}(a=r_g) \sim 0.3 M c^2 \sim 5 \times 10^{61} M_8 [\text{erg}] \quad (\text{pdV} \sim 10^{62} \text{ ergs required in clusters})$$

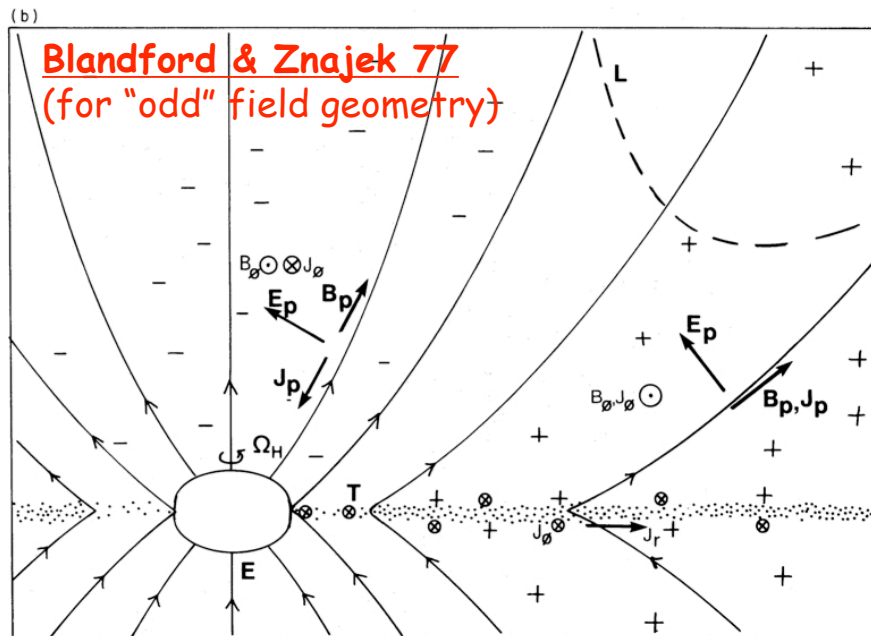
[scenario inspired by earlier developed models for young stars (Weber & Davis 67), pulsars (Michel 69, Goldreich & Julian 70), and accretion disks in active galaxies (Blandford 76, Lovelace 76, Bisnovatyi-Kogan & Ruzmaikin 76)]

- i) MF is dragged from outer distances and amplified by the accreting matter. It is assumed to be initially poloidal, aligned to the BH spin, supported by the toroidal currents within the accretion disk, with the intensity $B \sim B_E$ close to the event horizon.
- ii) Due to the frame-dragging effect, MF in the ergosphere is forced to rotate with the angular velocity $\omega \sim \Omega_S (r_S / r)^3$ as measured by ZAMO. Quadrupole poloidal EF is thus induced (in every frame) in the vacuum above the BH surface.
- iii) This vacuum is unstable for the pair creation. The created pairs accelerated by the aligned EF initiate electromagnetic cascades (curvature, synchrotron, and IC emission). In this way the force-free magnetosphere is established.
- iv) Charge distribution formed in the magnetosphere supports poloidal EF, and the generated currents create the additional poloidal and toroidal MF components.
- v) The combination of the poloidal EF and the toroidal MF leads to the radial Poynting flux which carry away energy. The combination of the poloidal EF and MF carries away angular momentum of the Kerr BH.

Blandford-Znajek Process



Steady-state, force-free character of the magnetosphere is anticipated (and $J/J_{\max} \ll 1$ is assumed). This implies that currents must flow along magnetic surfaces. These currents must be carried out and return along the field lines after passing through a region where force-free approximation breaks down sufficiently for the currents to cross the field lines. In this way plasma currents close an electric circuit around the BH equator and poles, enabling to extract energy at the maximum rate $L_{\text{BZ}} \sim P$.



$$\vec{E} \cdot \vec{j} = 0$$

$$Q\vec{E} + \frac{1}{c}\vec{j} \times \vec{B} = 0$$

relativistic
force-free

$$L_{\text{BZ}} = \frac{c}{32} \omega_{\text{F}} \left(\frac{J}{J_{\max}} \right)^2 B_r^2 r_{\text{S}}^2$$

(L_{BZ} dissipated "on the surface at infinity" depend on the match between the resistance at the BH surface and the resistance at the infinity. The anticipated "best match" $\mathfrak{R} \sim \mathfrak{R}_{\text{inf}}$ corresponds to the angular velocity of the field lines relative to that of the BH $\omega_{\text{F}} \sim 1/2$.)

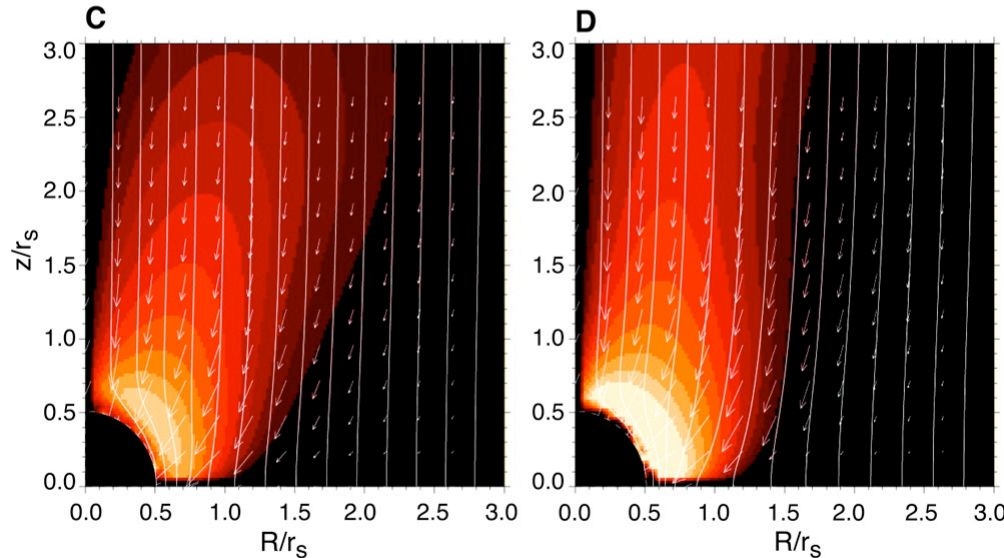
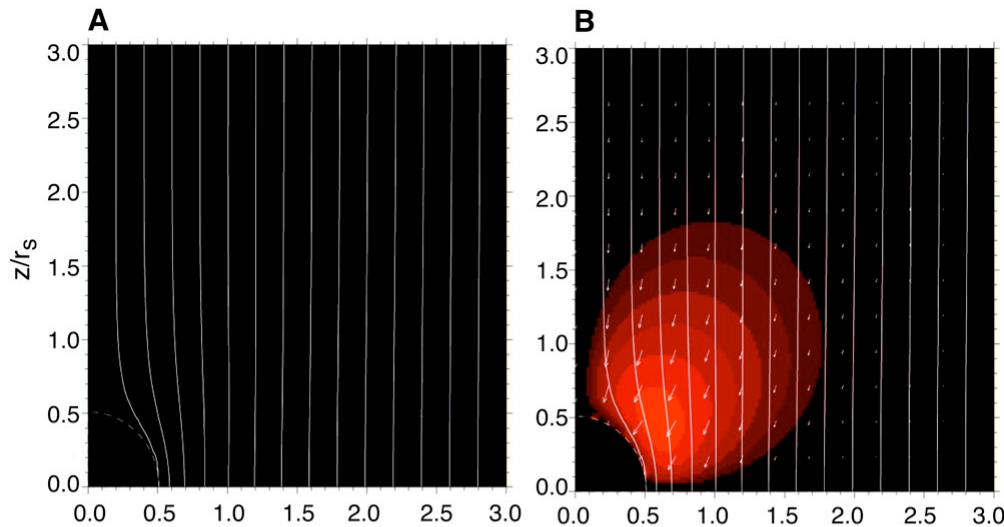
Is It Really Working?

- Does the force-free steady-state magnetosphere really form around Kerr BH embedded in an external MF?
- Is the perturbative solution provided by Blandford & Znajek for slowly rotating BH with split-monopole MF configuration stable? Is it valid for $J/J_{\max} \sim 1$?
- How realistic is the initial MF configuration anticipated by Blandford & Znajek for the accretion disk? Is strong ($\sim B_E$) poloidal magnetic field threading the BH ergosphere indeed expected?

(Punsly & Coroniti 90, Ghosh & Abramowicz 97, Livio+ 99)

These questions can be addressed by means of MHD numerical simulations of an accreting plasma in a strong gravity of a rotating SMBH!

First GR MHD Simulations



Kato, Koide, Kudoh, Meier, Shibata, Uchida: GR ideal MHD simulations of rapidly ($a/r_g > 0.9$) rotating BH embedded in a strong uniform magnetic field aligned to the BH spin and cold $\beta_M < 1$ plasma; no accretion disk; simulations relatively short ($\sim 10 r_g$).

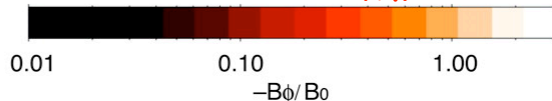
Cold plasma quickly starts to free-fall into the BH, and the MF lines start quickly to be azimuthally twisted by the differential rotation close to the BH critical surface (although do not cross the event horizon). This generates rapidly growing toroidal MF component in the equatorial plane of the ergosphere (frame-dragging effect). The twist of the MF lines propagates outward as a torsional Alfvén wave along the field lines against the in-falling plasma flow. Meanwhile, due to the magnetic tension force of the twisted MF, plasma in the ergosphere is torqued in the direction opposite to the BH spin, acquiring thus negative angular momentum (and energy).

Koide+02

toroidal MF

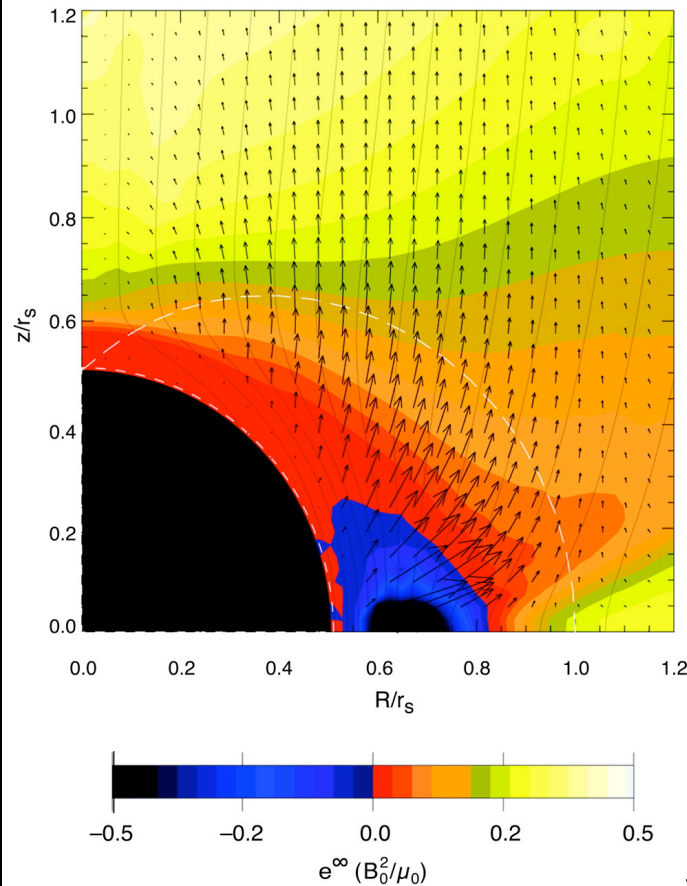
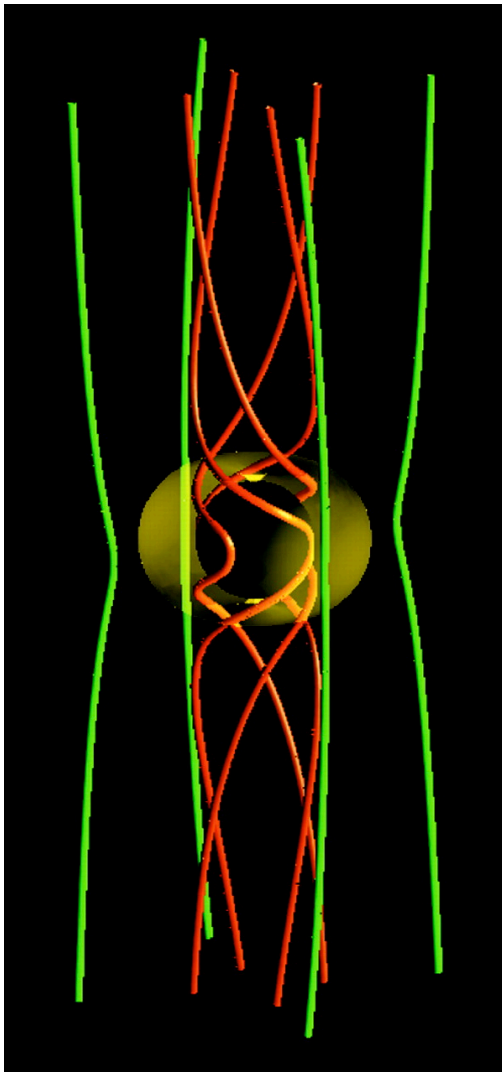


C

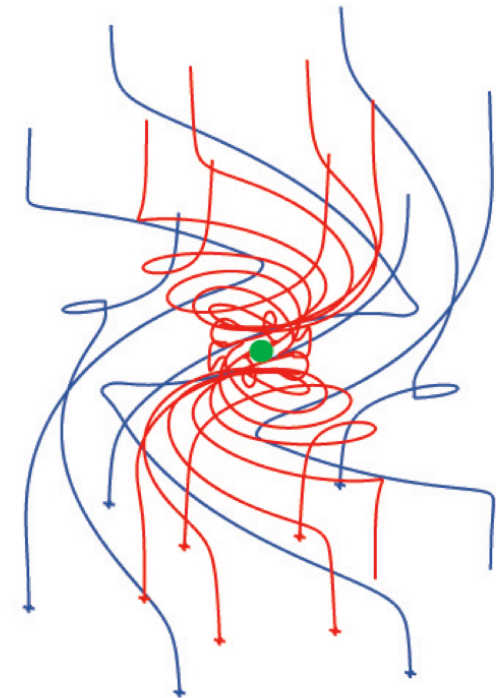


"MHD Penrose" Process

When the negative-energy plasma enters the event horizon, the EM energy is released (in a form of the torsional Alfvén wave) from the ergosphere in the expense of the BH rotational energy. This outflowing rotating helical MF coil drives the plasma trapped in it upward along the field lines. The Lorentz force $\mathbf{j} \times \mathbf{B}_T$ collimates and accelerates the outflow further out.



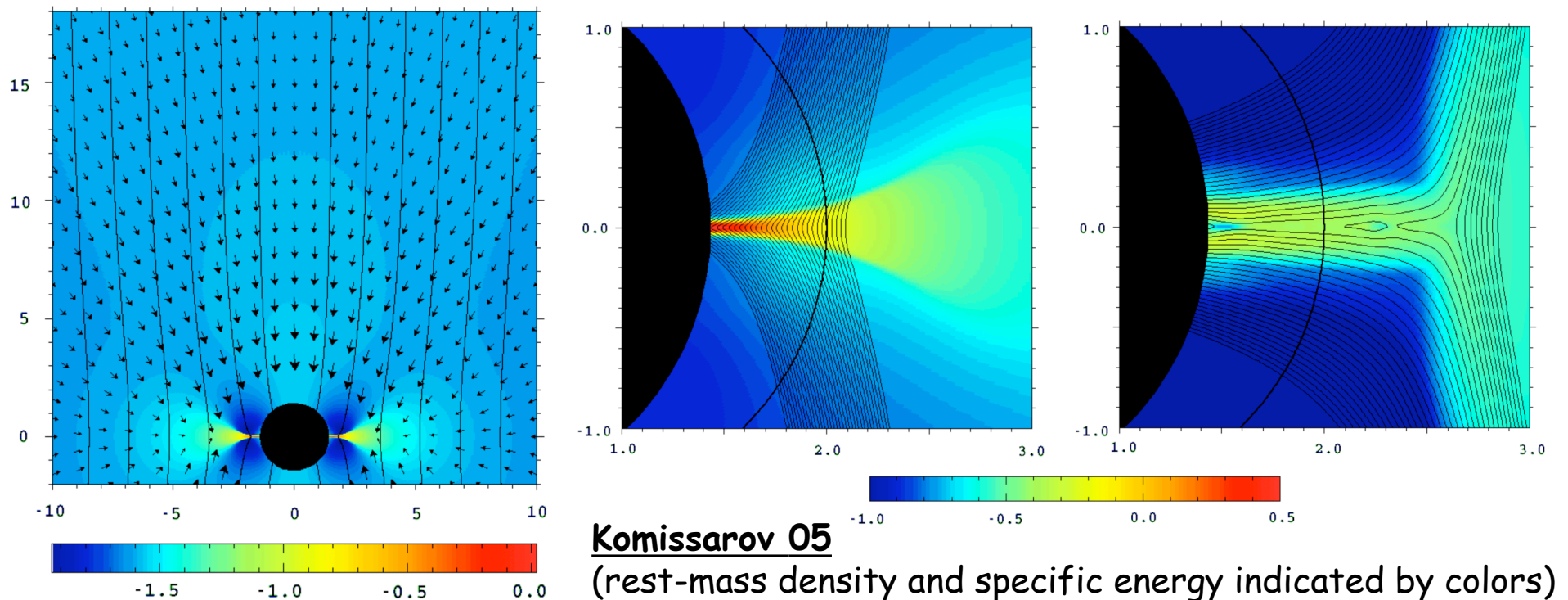
Koide+02: MF lines; EM energy flux density.



The same process was observed in longer ($>10 r_g$) simulations by **Mizune, Nishikawa & Hardee 07** (axisymmetric GR ideal MHD, BL coordinates, thin disk not supporting MRI added).

EM Effects At Work

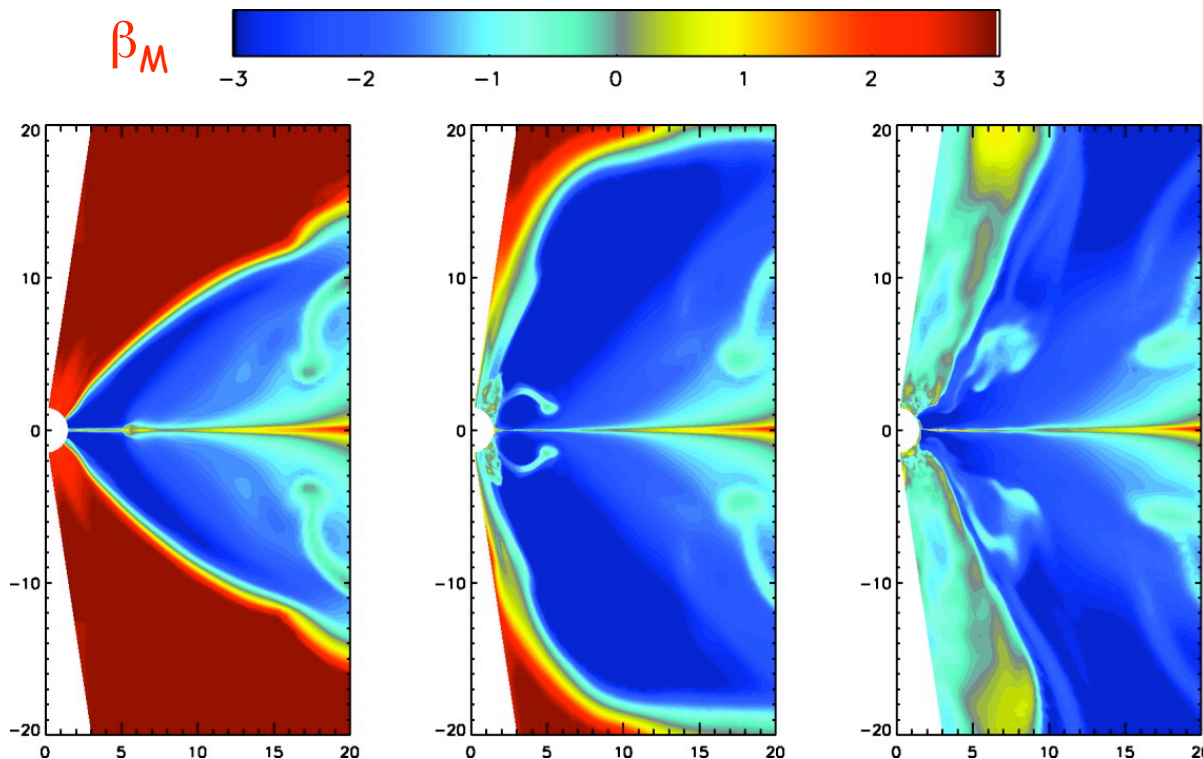
Komissarov: GR force-free simulations of a rapidly ($a/r_g > 0.9$) rotating BH embedded in a cold $\beta_M < 1$ plasma and a strong uniform magnetic field aligned to the BH spin; no accretion disk; relatively long simulations ($\sim 100 r_g$); anisotropic resistivity added.



Initially, the results agree with those obtained by Koide et al. However, after some time ($> 10 r_g$) the dissipative current sheet forms within the ergospheric disk re-organizing MF lines which, at some point, enter the event horizon. Thus, the split-monopole MF configuration is spontaneously established, and the MHD Penrose process evolves toward the BZ model. The BZ solution occurs to be stable. **No jet is present in the simulations.**

BH-Torus Simulations

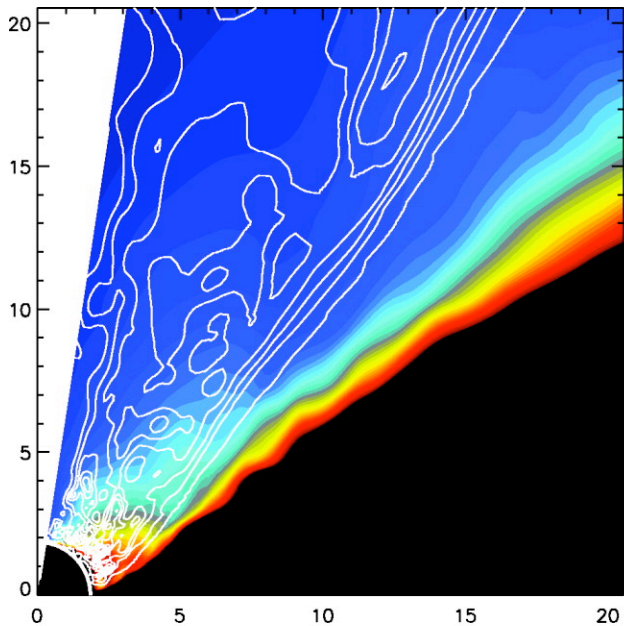
Hawley, Krolik, De Villiers, Hirose: 3D non-conservative GR ideal MHD simulations of a long-term ($\sim 10^4 r_g$) evolution of an isolated gaseous torus orbiting rapidly ($a/r_g > 0.9$) rotating BH with no initial large-scale magnetic field; BL coordinates.



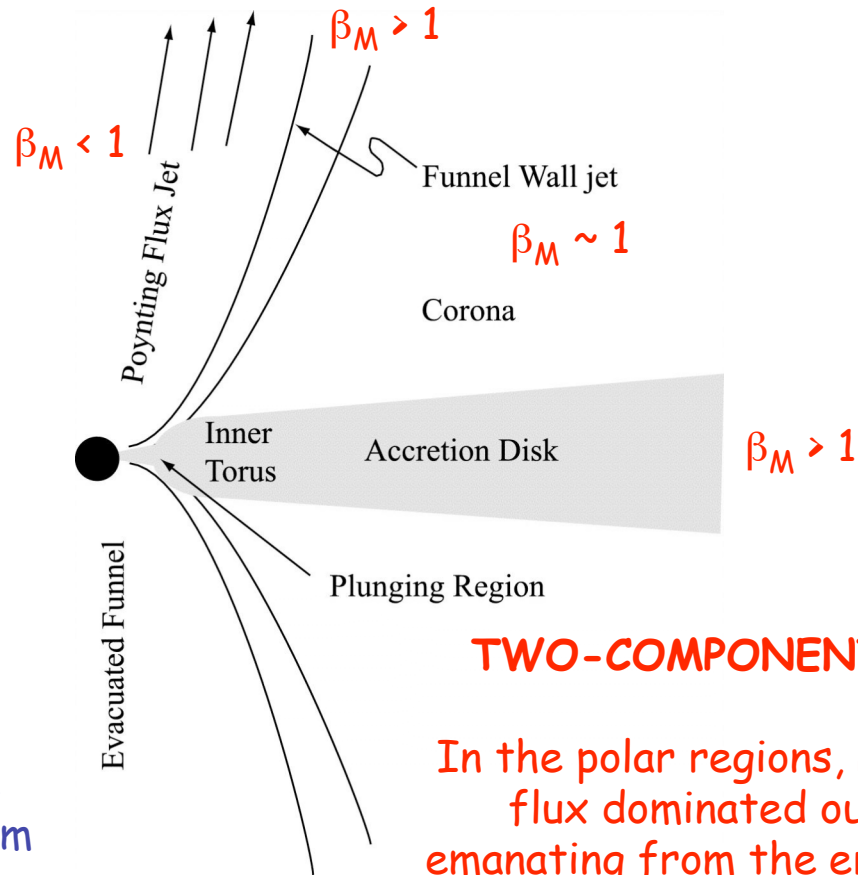
Magnetic tower (as seen by Koide et al.) is quickly generated when the accreting matter reaches the event horizon due to a strong magnetic pressure gradient which builds up and drives the plasma upward. This evolves later toward a slow ($v/c \sim 0.3$) "funnel-jet".

Hawley & Krolik 06: The torus is initially supported against the gravity by pressure and rotation, and the polar regions above the BH are initially empty due to centrifugal forces and no initial MF assumed. Small loops of a weak poloidal MF added at the beginning to the torus ($\beta_M \sim 100$), which then becomes unstable for MRI and thus turbulent. The small-scale MF starts to be then amplified (forming large scale poloidal MF component), angular momentum starts to be transported, and the accretion begins through the "plunging region". Above the surface of the disk, a hot corona ($\beta_M \sim 1$) is immediately established.

Two-Component Outflows



Hawley & Krolik 06: total pressure indicated by colors; radial momentum flux indicated by contours



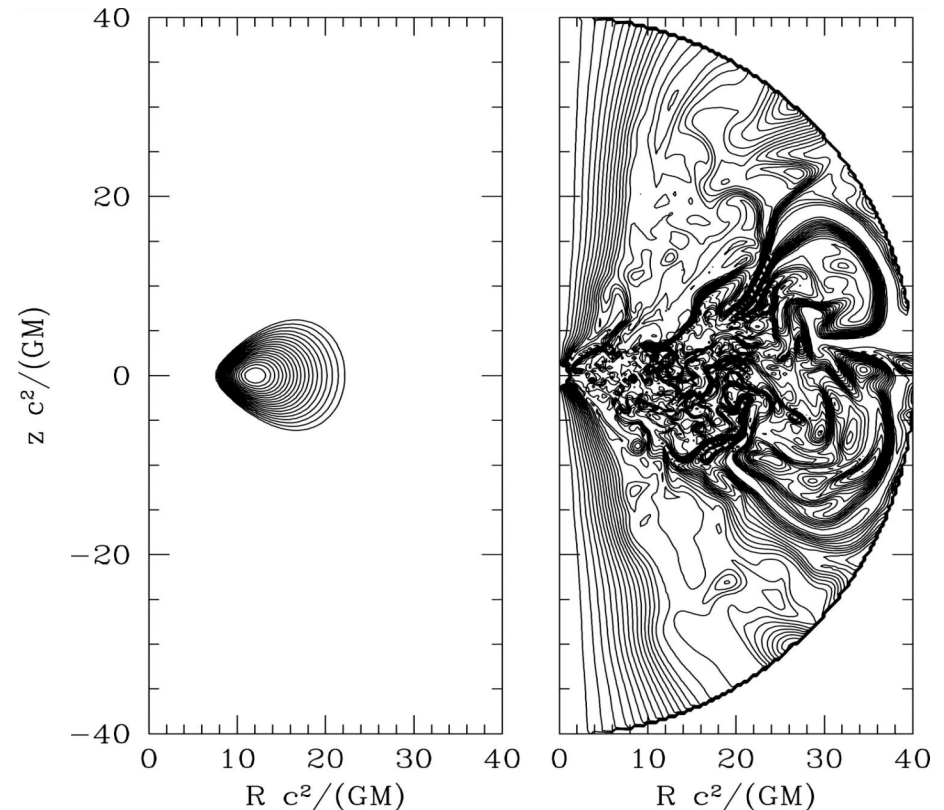
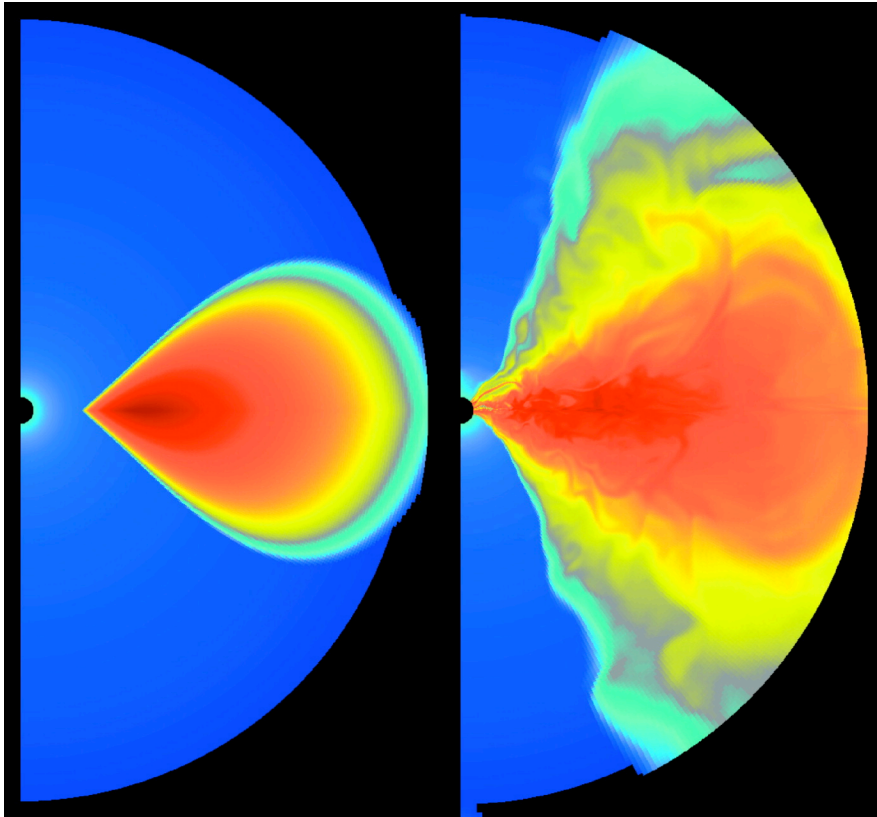
TWO-COMPONENT JET:

In the polar regions, Poynting-flux dominated outflow emanating from the ergosphere is observed ("BZ jet"). It is surrounded by the matter-dominated funnel jet. Both outflows are collimated by the torus and corona pressures.

Large-scale MF involved in the energy extraction from rotating BH is not assumed, but created self-consistently by the accreting matter. The power of the outflow relative to the accretion rate (as well as a relative strength of the central and funnel jets) is a strong function of the BH spin.

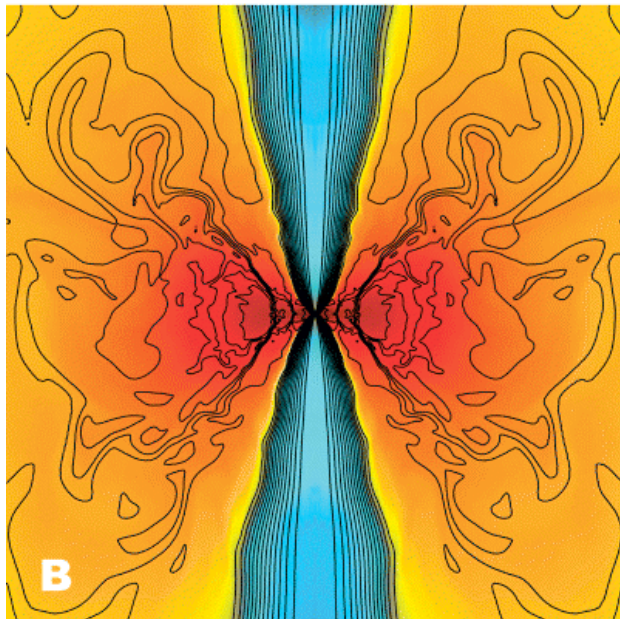
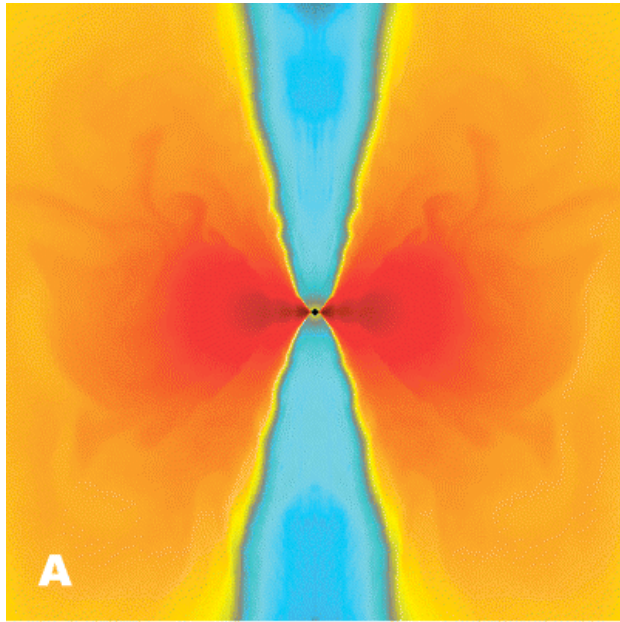
EM Jets

McKinney, Gammie: axisymmetric conservative GR ideal MHD simulations of a long-term ($\sim 10^4 r_g$) evolution of an isolated gaseous torus orbiting rapidly ($a/r_g > 0.9$) rotating BH with no initial large-scale magnetic field; modified KS coordinates.



McKinney & Gammie 04 (rest density indicated by colors; poloidal magnetic field indicated by contours): results very similar to those obtained by Hawley et al. In particular, a two-component outflow with a force-free relativistic ($v \sim c$) spine and a matter-dominated slow ($v \sim 0.75 c$) outer sheath/wind is observed. Little mixing between these two components noted.

Evolution of the EM Jet



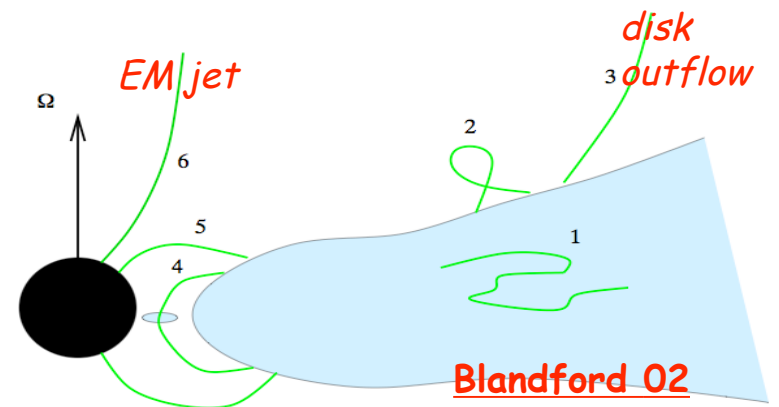
McKinney 06: outflow on a scale of $10^2 r_g$ (density indicated by colors, magnetic field by contours).

Domination of an ordered poloidal field component up to $\sim 10^3 r_g$ within the central, Poynting-dominated outflow. Up to these distances from the BH, the central jet spine accelerates and collimates along nearly paraboloidal field lines. Beyond, the toroidal field dominates, and the central outflow experiences pinch instabilities. These instabilities cause poloidal oscillations which drive waves that may steepen to shocks. Such shocks convert magnetic energy to the thermal one - the jet at this point stops being accelerated, and becomes conical with the opening angle of ~ 5 deg. (Axisymmetric simulations, so no kink modes included)

Jet Launching - Summary

WHAT (WE THINK) WE KNOW:

- The Bladford-Znajek model for extraction of the BH rotational energy in a form of a Poynting-dominated outflow is correct and stable (Komissarov, Koide et al., Mizuno et al.).
- Large-scale poloidal MF (of a split-monopole configuration) involved in the energy extraction need not be assumed, since it is expected to be self-consistently generated by MRI operating in accretion disk (Hawley & Krolik et al., McKinney & Gammie).
- Launched jets are expected to be two-component, with a central e+e- force-free spine (dominated by the poloidal MF up to distances $10^3 r_g$, toroidal MF further away) and a matter-dominated sheath.
- The accessible jet power and its strong dependence on the BH spin both seem to be consistent with the observations of AGNs ("spin paradigm"; see **Sikora et al. 2007**).



WHAT WE DO NOT KNOW:

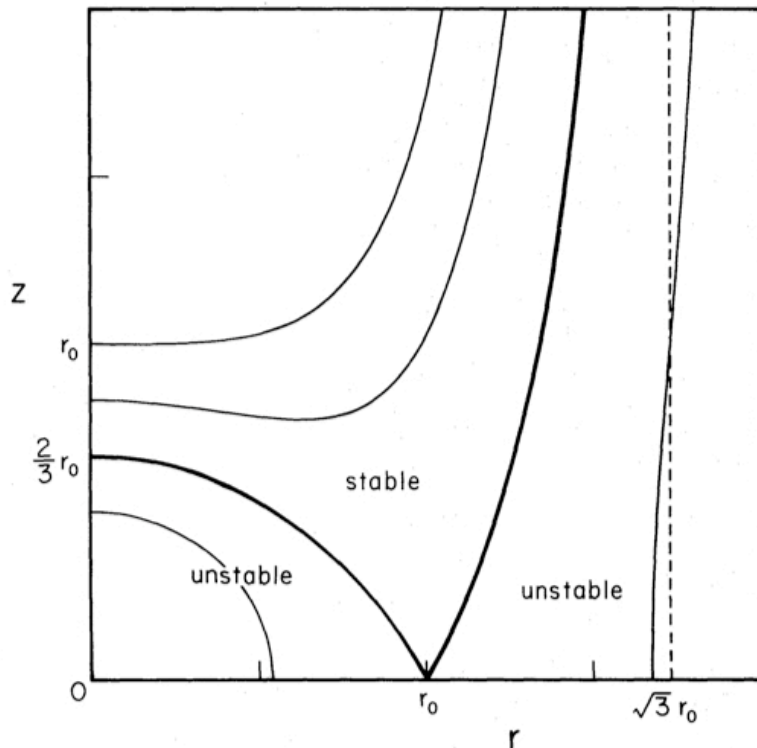
- How sensitive is the jet production with respect to the properties of the accretion disk, and in particular its detailed magnetic field structure?
- What is a role/importance of the outer wind launched from the accretion disk? Can it dominate over the Blandford-Znajek outflow?

Disk Outflows

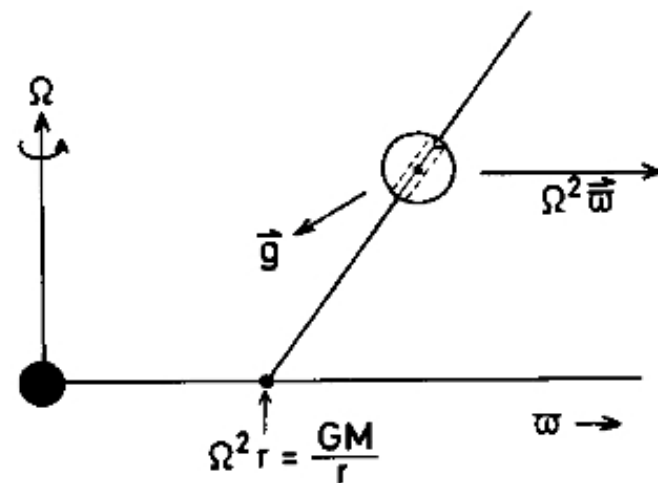
Open poloidal MF lines that leave the surface of a heavy thin accretion disk and extend to large distances can extract the energy and angular momentum of the accreting matter.

$$\Phi_{\text{cg}} \equiv \Phi_{\text{grav}} - \frac{1}{2}\Omega^2 r^2 = -\frac{GM}{r_0} \left[\frac{1}{2} \left(\frac{r}{r_0} \right)^2 + \frac{r_0}{\sqrt{r^2 + z^2}} \right]$$

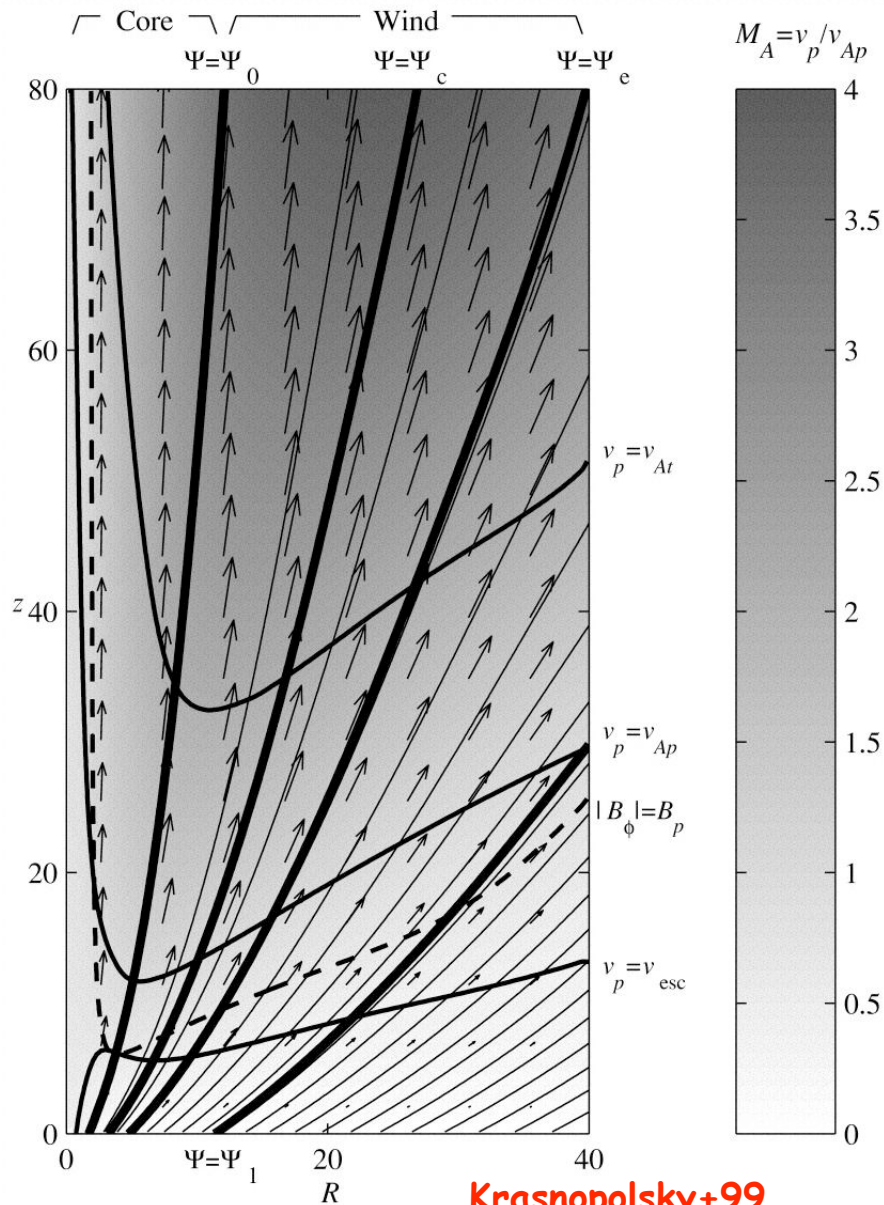
The centrifugal-gravitational potential is decreasing along the MF lines inclined $< 60^\circ$ to the disk surface (for Newtonian gravity and Keplerian rotation; **Blandford & Payne 82**).



Dynamically dominating matter within the disk forces the frozen-in open poloidal MF lines to rotate, say, at the local Keplerian angular velocity $\Omega = (GM / r_0^3)^{1/2}$, where r_0 is the radius of a footpoint for a given line. Since charged particles (both protons and electron-positron pairs) can easily leave the accretion flow, one should expect a low-density magnetosphere to be generated above the disk surface.



Blanford-Payne Process



Blandford & Payne 82: axisymmetric cold magnetosphere and open poloidal MF lines are present above the surface of the Keplerian disk ($\rho_d \propto r^{-1/2}$, $B_d \propto r^{-5/4}$). MF lines supported by the disk are anchored in and co-rotating with the accreting matter. An outflow of magnetized plasma is centrifugally driven from the disk surface (with the mass loss rate from each decade of the disk radius being independent on r) along the MF lines (fluid elements are moving along the MF lines “like a bead on a rotating wire”).

Note that this is the tension and pressure gradient of the MF modified by the rotation within the magnetosphere (due to the generated toroidal MF component) which determines the acceleration of the fluid elements along the poloidal MF lines (in the inertial frame centrifugal forces becomes magnetic ones; see **Spruit 96**).

NR, Ideal, & Axisymmetric MHD

$$\vec{\nabla} \cdot (\rho \vec{v}) = 0$$

$$\vec{\nabla} \times (\vec{v} \times \vec{B}) = 0$$

$$\vec{v} \cdot \vec{\nabla} (p/\rho^{\hat{\gamma}}) = 0$$

$$\rho (\vec{v} \cdot \vec{\nabla}) \vec{v} = -\vec{\nabla} p + \frac{1}{4\pi} (\vec{\nabla} \times \vec{B}) \times \vec{B} - \rho \vec{\nabla} \Phi_{\text{grav}}$$

Ideal steady-state MHD

$$\vec{B}_P = B_r \hat{r} + B_z \hat{z} = -\frac{\hat{\phi} \times \vec{\nabla} \Psi}{r}$$

$$\vec{B}_T = B_\phi \hat{\phi},$$

Poloidal and toroidal MF components defined through the magnetic flux function Ψ

Surface functions: $(\vec{B} \cdot \vec{\nabla}) f = 0$

axisymmetry \rightarrow Grad-Shafranov equation plus several surface functions:

$$k = \frac{\rho v_P}{B_P}$$

mass loading

$$\Omega = \frac{v_\phi}{r} - \frac{k B_\phi}{r \rho}$$

angular velocity

$$\ell^* = r v_\phi - \frac{r B_\phi}{4\pi k}$$

specific angular momentum

$$\varepsilon^* = \frac{1}{2} v^2 + \frac{\varepsilon + p}{\rho} - \frac{r \Omega B_\phi}{4\pi k} + \Phi_{\text{grav}}$$

specific energy

$$s = \frac{p}{\rho^{\hat{\gamma}}}$$

specific entropy

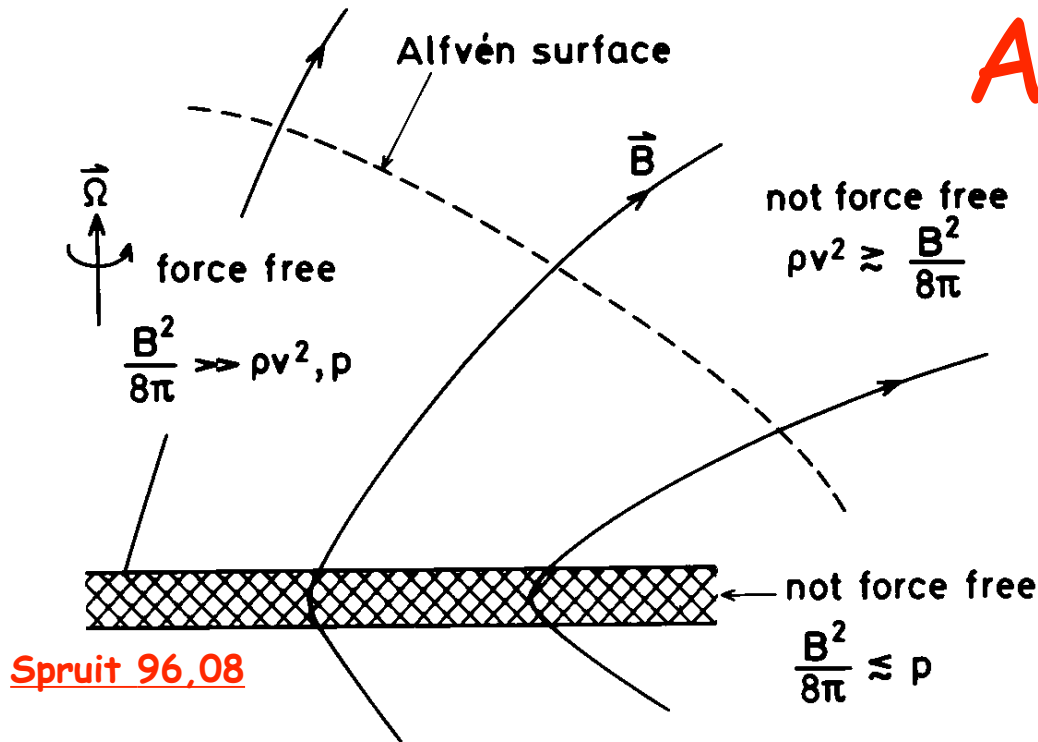
General But Difficult...

The problem is very general, since it applies to outflows produced in protostellar objects, gamma-ray bursts, pulsar wind nebulae, and active galaxies. However, the Grad-Shafranov equation is in general very complicated mathematically, and in addition it becomes singular at several critical points/surfaces whose loci are unknown a priori where the fluid velocity equals the speed of backward-propagating disturbances (slow, Alfvén, and fast magnetosonic waves). Physical solutions must, of course, cross the critical surfaces smoothly, and such conditions determines some free constants of the solved equations.

Many particular solutions to the discussed problem were presented in the literature. They differ in the additional assumptions involved (initial configuration of the poloidal MF, self-similarity, wind radial stratification, relativistic vs. non-relativistic flow velocities, etc.). The analytical and numerical investigations were presented in, e.g.:

Blandford & Payne 1982; Sakurai 1985, 1987; Camenzind 1986, 1987; Lovelace 1986, 1987, 1989; Konigl 1986, 1989; Heyvaerts & Norman 1989, 2003; Chiueh et al. 1991, 1998; Li & Begelman 1992; Li 1993; Appl & Camenzind 1993; Contopoulos 1994, 1995; Contopoulos & Lovelace 1996; Bogovalov 1992, 1994, 1995, 1996, 2001; Spruit 1996; Beskin et al. 1998; Sauty & Tsinganos 1994; Romanova et al. 1997; Ustyugova et al. 1999; Krasnopolsky et al. 1999; Bogovalov & Tsinganos 1999, 2001, 2005; Tsinganos & Bogovalov 2000, 2002; Vlahakis & Tsinganos 1998, 1999, 1997; Vlahakis et al. 2000; Vlahakis & Konigl 2003, 2004; Beskin & Nokhrina 2006; Komissarov et al. 2007.

Alfven Surface



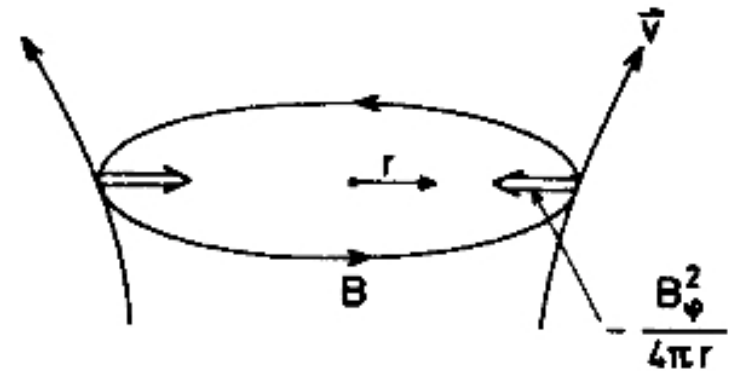
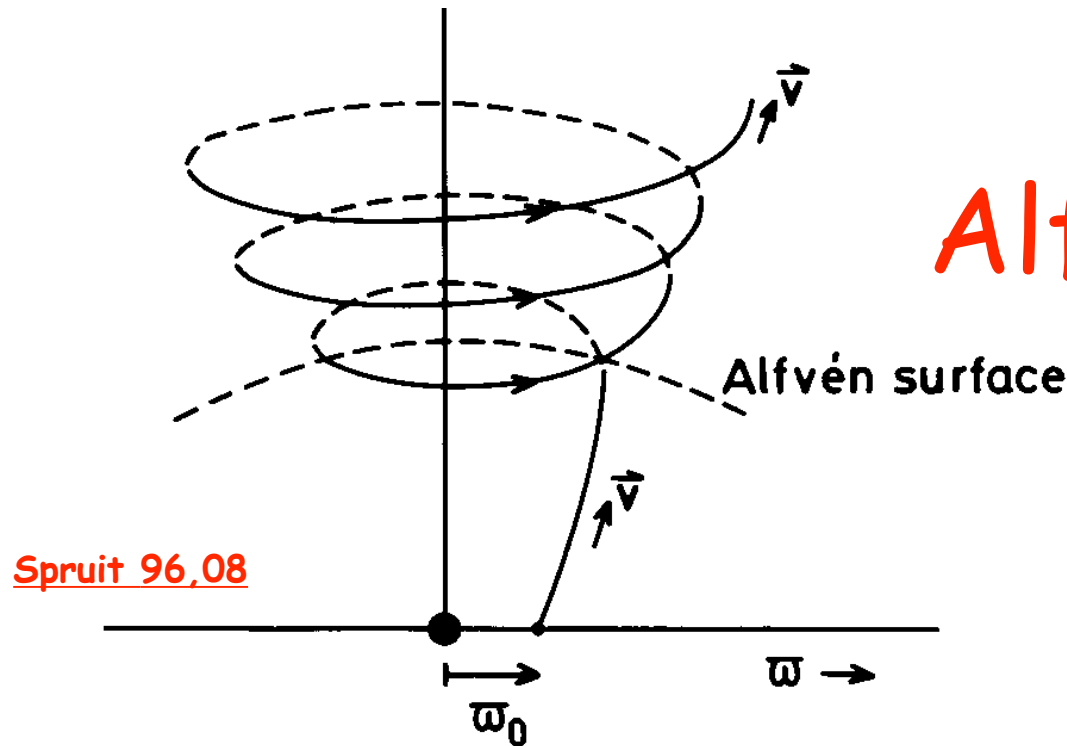
Michel's magnetization parameter (essentially the ratio of Poynting and inertial fluxes):

$$\sigma_M \equiv \frac{\phi_M^2 \Omega^2}{4\dot{m}c^3} = \left(\frac{v_A^P}{c}\right)^2 \left(\frac{r}{R_L}\right)^2 \left(\frac{v_p}{c}\right)^{-1}$$

where $\phi_M = B_P r^2$ is the poloidal magnetic flux, $\dot{m} = \pi \rho v_P r^2$ is the mass flow rate, and $\Omega = c/R_L$.

The open MF lines purely poloidal initial configuration are forced to co-rotate with the high- β_M disk, while the matter is centrifugally driven outward into the low- β_M corona and moves along the open field lines. When the velocity of the fluid approaches the poloidal Alfven velocity, $v_p = v_{A,p} \equiv B_p / (4\pi\rho)^{1/2}$ (i.e., near the Alfven surface R_A), the matter cannot be accelerated by the centrifugal forces anymore. Note that the relativistic velocities at the Alfven surface can be reached only if the Alfven speed is relativistic itself, i.e. if the magnetospheric plasma is highly magnetized, and the Alfven radius approaches the light cylinder $R_L = c/\Omega$. Note also that the force-free approximation, which may be valid in between the disk and the Alfven surfaces, is obviously violated around and beyond the later critical surface.

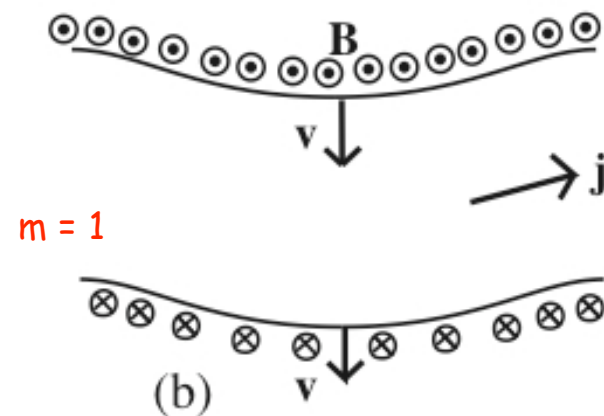
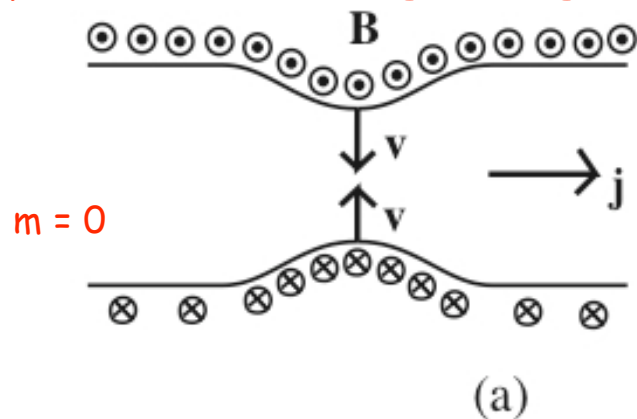
Beyond Alfvén Surface



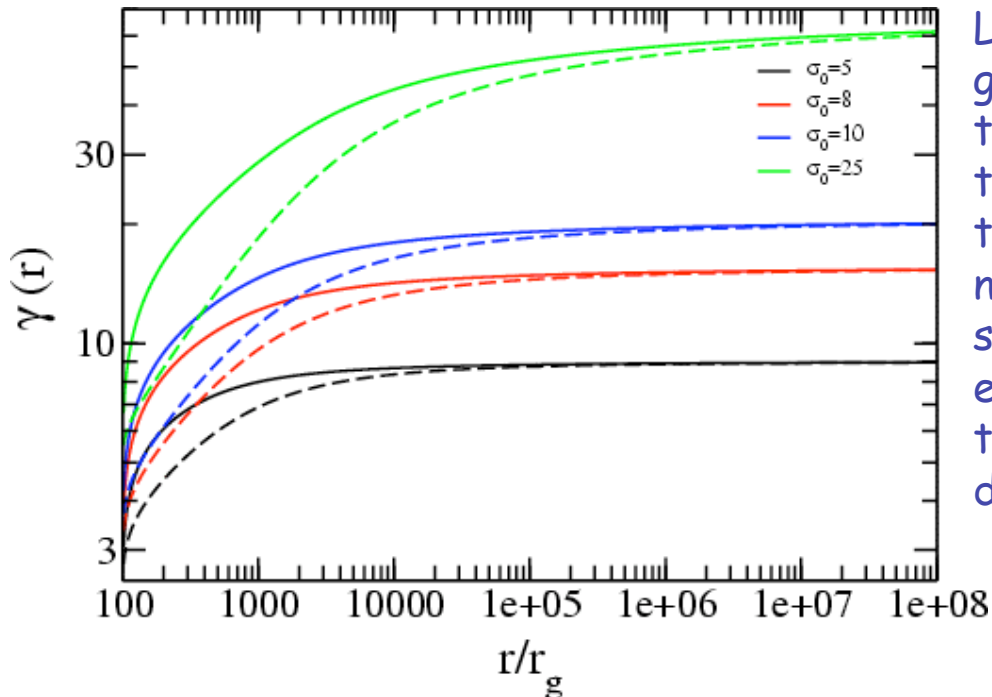
Beyond the Alfvén surface the poloidal MF is not strong enough to enforce the co-rotation. Instead, inertia of the matter becomes important, and the gas starts to wind up the MF lines, forming the spiral shape beyond the Alfvén surface. Such toroidal MF created by the backward twisting of the rotating poloidal component becomes dominant at further radii (relatively close to the Alfvén surface, however) near the rotation axis. **Note that by virtue of the Ampere's law, this configuration carries a poloidal current.** Meanwhile, the curvature force of the toroidal field collimate the outflow by compressing the outflowing matter toward the jet axis ('hoop stresses') due to the $\mathbf{j} \times \mathbf{B}_T$ force (note that the currents flow along the magnetic surfaces). Such collimation induces a reduction in the poloidal MF flux along the poloidal streamlines, i.e. a reduction of the Poynting flux along the flow. Because of this, the gradient of the MF pressure associated with the toroidal field drives further acceleration of the outflow beyond the Alfvén surface up to the fast magnetosonic surface R_F (where $v_p = v_{A,tot} \equiv B_{tot} / (4\pi\rho)^{1/2}$), increasing the plasma kinetic energy along the jet.

KH and CD Instabilities

- Jets are subjected to Kelvin-Helmholtz (KH) instabilities, for which the source is a relative kinetic energy between the outflow and the ambient medium. Relativistic velocities and longitudinal MF (if strong enough) may stabilize an outflow (Birkinshaw 91, Hardee 07, Perucho+07).
- Magnetized jets collimated by toroidal MF are also subjected to current-driven (CD) Z-pinch instabilities. These may re-arrange MF configuration, leading to disruption of an outflow and enhanced energy dissipation (Appl & Camenzind 92, Eichler 93, Spruit+97, Begelman 98, Lyubarsky 99, Nakamura & Meier 04)
- Dominant modes of the Z-pinch instabilities are kink ($m=1$) and pinch ($m=0$) ones. They may be stabilized by the large-scale longitudinal MF component (if strong enough).



A Role of Kink Instabilities



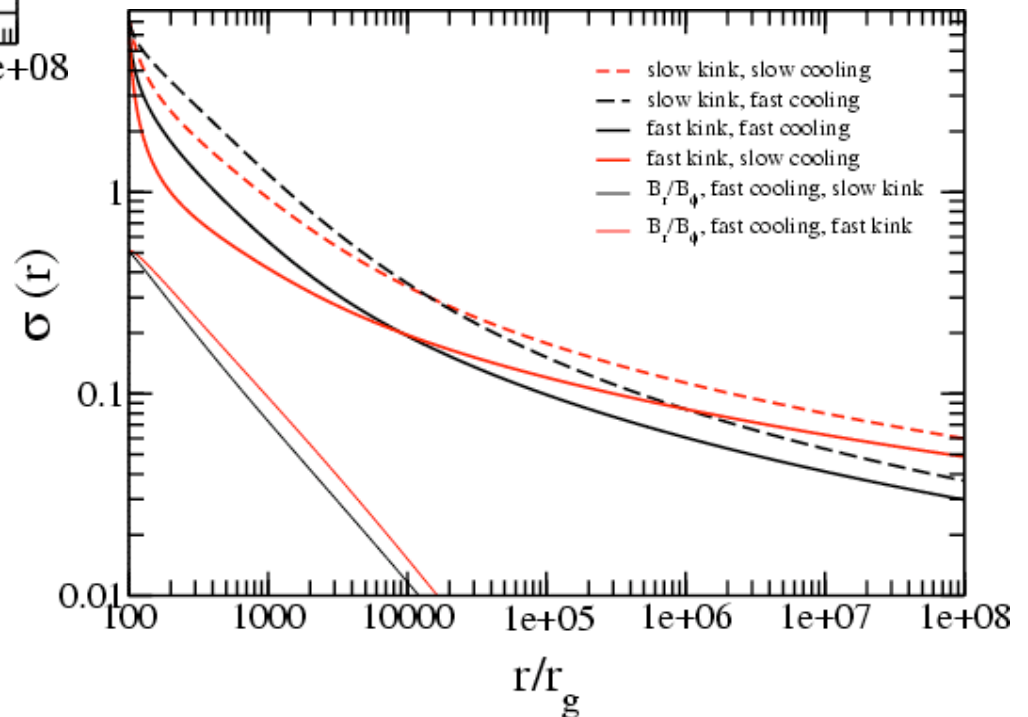
Linear analysis indicates that kink instabilities grow on the Alfvén crossing timescale across the outflow in a comoving frame. If this timescale is shorter than the jet expansion timescale, kink instabilities grow rapidly. The non-linear growth is expected to provide a sink for the toroidal MF. The magnetic energy extracted in this way may accelerate further the outflow and lead to the enhanced energy dissipation.

Giannios & Spruit 06: jet acceleration due to the developing kink instabilities proceeds until the flow becomes completely matter-dominated; this is expected at:

$$r \sim (10-100) R_F \sim (10^3-10^4) r_g$$

The resulting terminal bulk Lorentz factor:

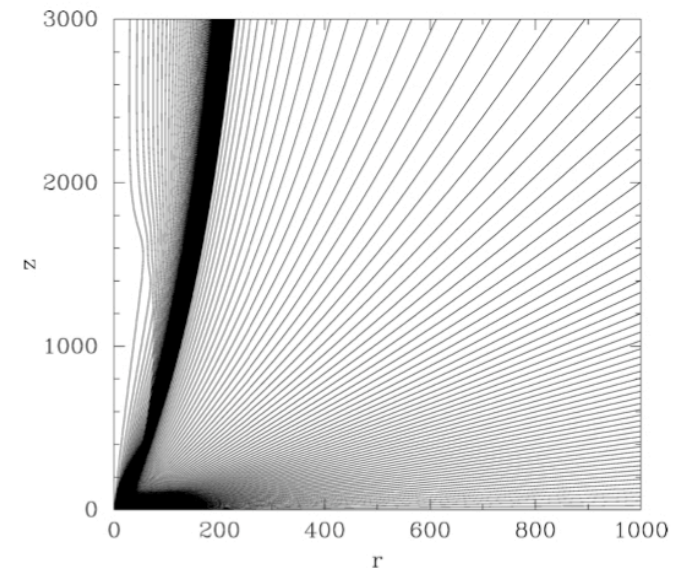
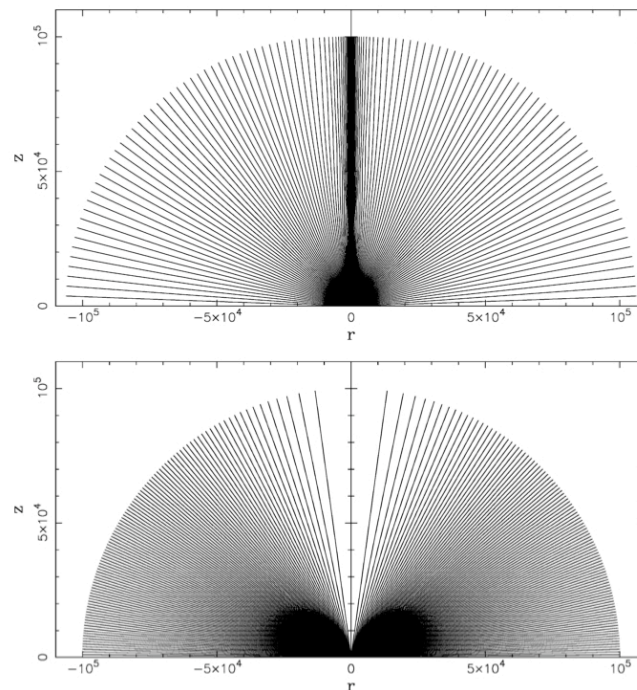
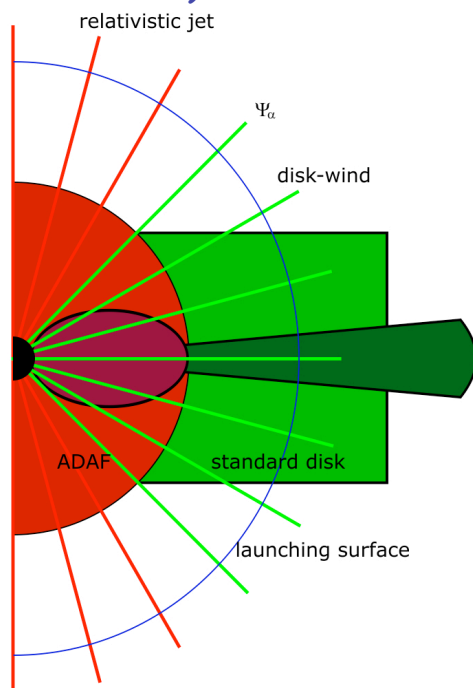
$$\Gamma \sim (L_{PF} / L_{kin})_{RF}$$



Low Efficiency?

Bogovalov & Tsinganos 02,05: efficiency of the jet formed in the Blandford-Payne process is very low, in a sense that the central collimated part of the wind constitutes a negligible ($< 1\%$) fraction of the total mass and magnetic flux outflowing from the disk. This is especially true in the relativistic regime $v \sim c$, when the electric field $\mathbf{E} = -(\mathbf{v}/c) \times \mathbf{B}$, inducing a force acting against the collimating $\mathbf{j} \times \mathbf{B}_T$ force, is of a comparable magnitude to the MF.

Possible solution: a two-component wind. For example (i) initially uncollimated but relativistic plasma outflowing from the inner portion of the accretion disk (e.g., of the ADAF structure)/SMBH with negligible (when compared to the outer wind) angular velocity and thus negligible toroidal magnetic field, plus (ii) non-relativistic wind with significant angular momentum emanating from the outer parts of the disk (of the standard Shakura-Sunayev structure).



Jet Formation - Summary

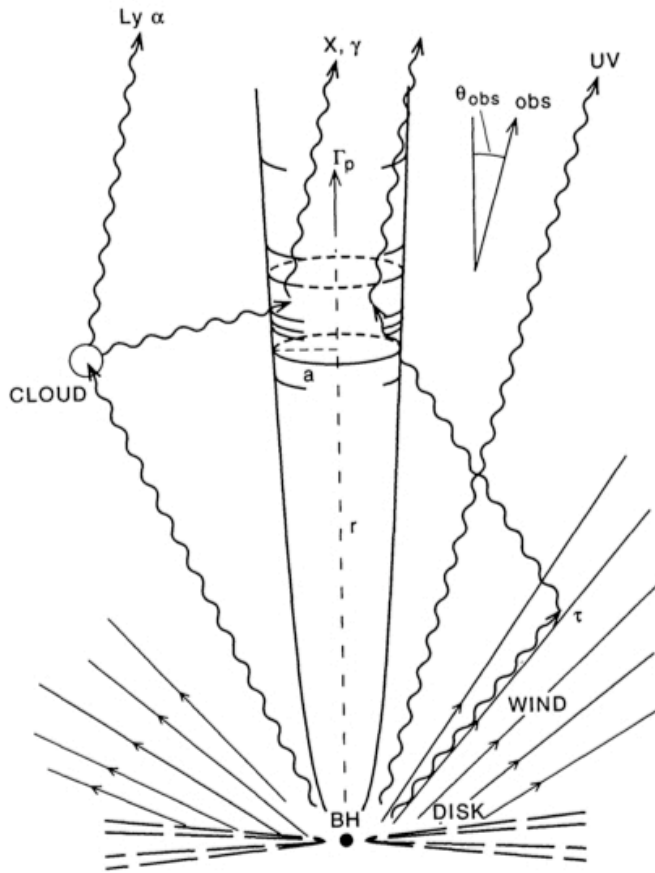
WHAT (WE THINK) WE KNOW:

- Formation of slowly collimating and accelerating outflows, gradually converting the Poynting flux to the kinetic one, is a general property of rotating accretion disks supporting open poloidal MF lines.
- Such outflows are expected to be composed of p+e- pairs, with the dominant toroidal MF from (basically) very beginning.
- The terminal velocity, the terminal opening angle, and the total power of thus formed jets are however rather model-dependent.
- For strongly magnetized AGN magnetosphere, outflow velocities are $v \sim v_{A,P} \sim c$ at the Alfvén surface $R_A \sim R_L \sim 10 r_g$. The jets accelerate then up to bulk Lorentz factors $\Gamma \sim \sigma_M^{1/3}$ at the fast magnetosonic surface $R_F \sim 100 r_g$.

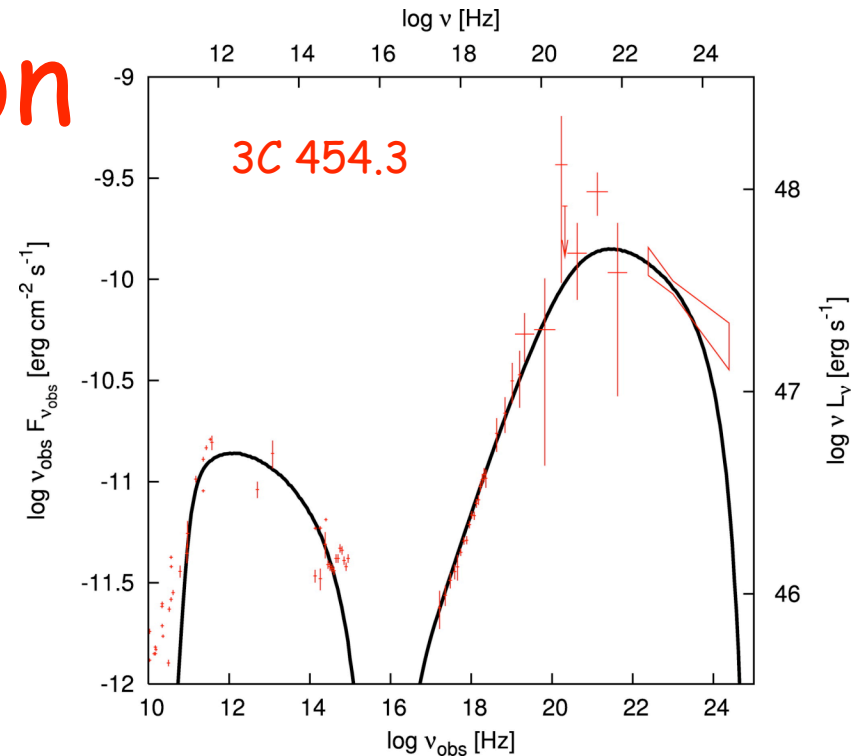
WHAT WE DO NOT KNOW:

- Is further acceleration and collimation possible beyond the fast magnetosonic surface (in the ideal homogeneous model) up to the maximum allowed $\Gamma \sim \sigma_M$ (Begelman & Li, Vlahakis & Königl, Beskin et al.)?
- Is this jet formation process efficient, especially in a relativistic regime (Bogovalov & Tsinganos)?
- What is a role of the kink and pinch (or also KH) instabilities (Begelman, Spruit, Hardee, Perucho)?
- Do the jets become matter-dominated at some point? Where exactly?
- Configuration of the accretion disk (SS vs. ADAF vs. ADIOS)

Blazar Phenomenon



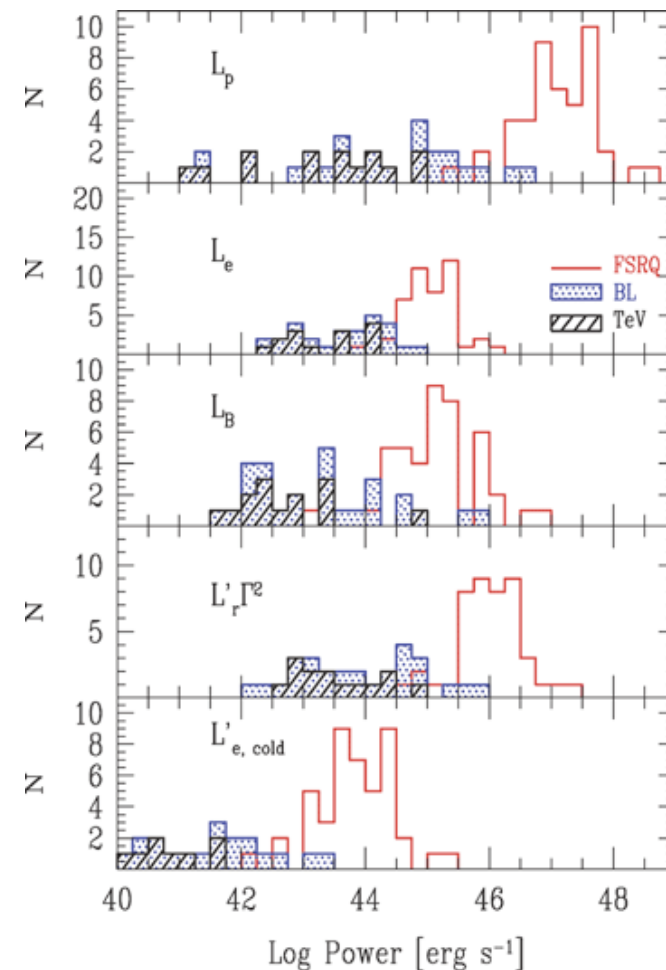
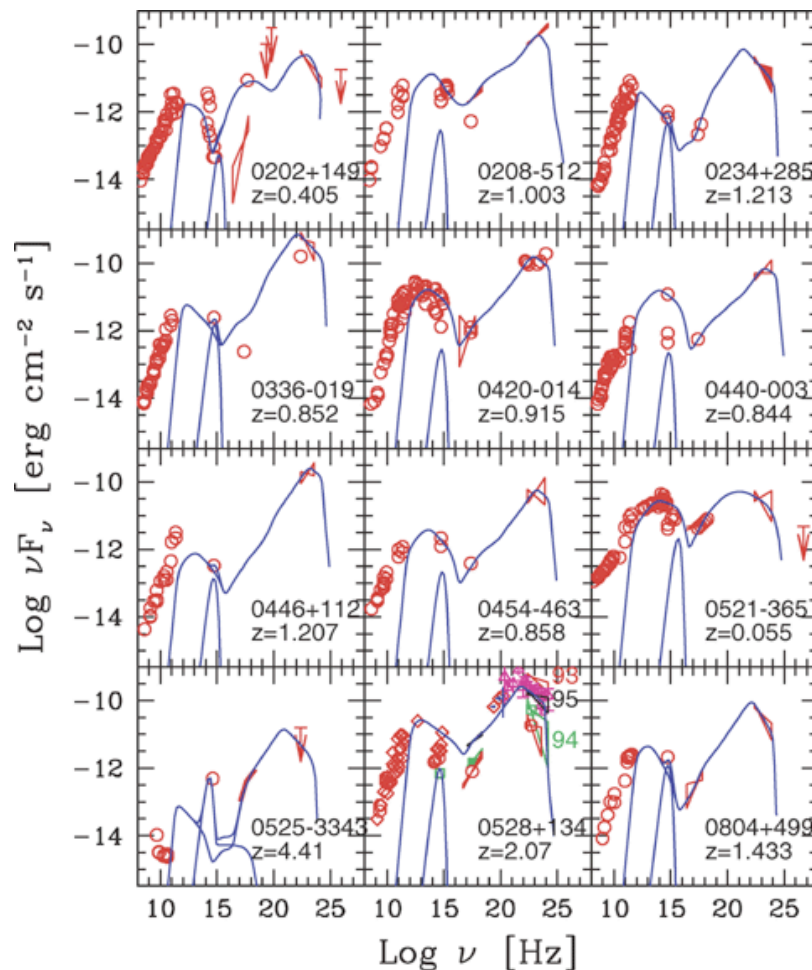
Modelling of the broad-band blazar emission (and its variability) in a framework of the leptonic scenario (**Sikora, Begelman & Rees 94**, **Blandford & Levinson 95**; but talk to **Alan Marscher!**) allows to put some constraints on the physical parameters of the blazar emission region. In particular, such modeling indicate that:



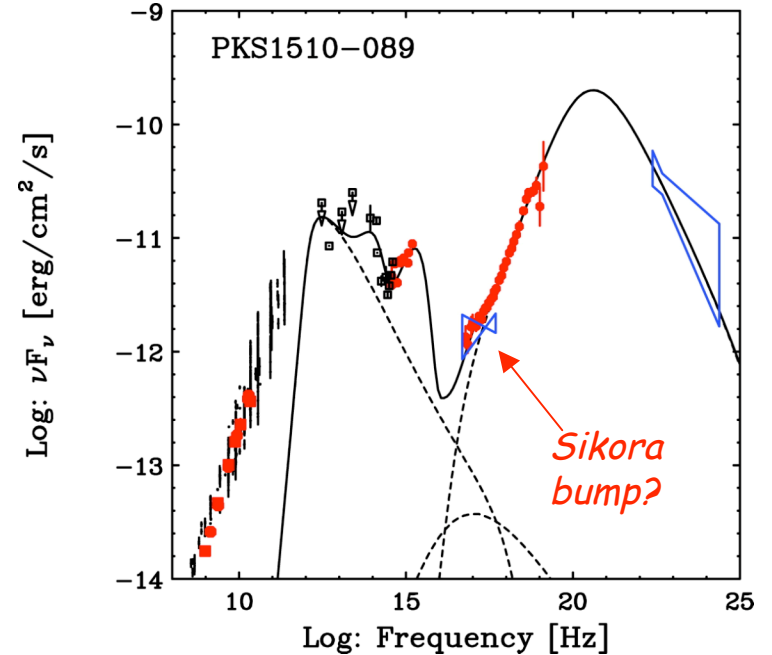
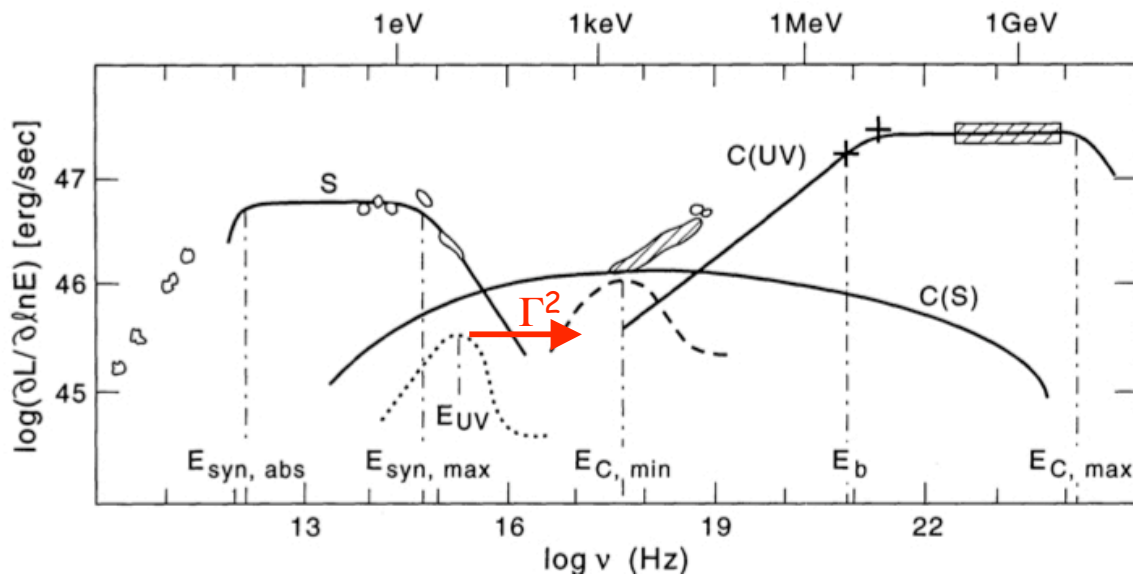
- 1) Emission regions are compact, $R \sim 10^{16} \text{ cm}$.
- 2) Implied highly relativistic bulk velocities of the emitting regions, $\Gamma \sim 10-30$, are in agreement with the ones inferred from the observed superluminal motions of VLBI jets on pc (kpc?) scales.
- 3) Energy density of MF is typically slightly below energy density of radiating ultrarelativistic electrons, $U_B \leq U_{e,rel}$.
- 4) The implied MF intensity $B \sim 0.1-1 \text{ G}$ is consistent with the one inferred from the SSA features in flat spectra of compact radio cores.

What Carries the Jet Power?

In addition, the power carried by ultrarelativistic electrons cannot account for the total radiated power of blazars, or for the kinetic power of quasar jets deposited far away from the active nucleus (e.g., Celotti & Ghisellini 08). So either (1) MF is dominating dynamically, while blazar emission is produced in small jet sub-volumes with MF intensity lower than average (magnetic reconnection?), or (2) jets on blazar scales are dynamically dominated by protons and/or cold electrons.



Where Is "Blazar Zone"?



GLAST is needed!

In the "internal shock model" (**Sikora, Begelman & Rees 94, Spada+01**) one should expect blazar emission zone located at the distances $r \sim \Gamma^2 r_g \sim (10^2 - 10^3) r_g \sim 0.01-0.1 \text{ pc}$.

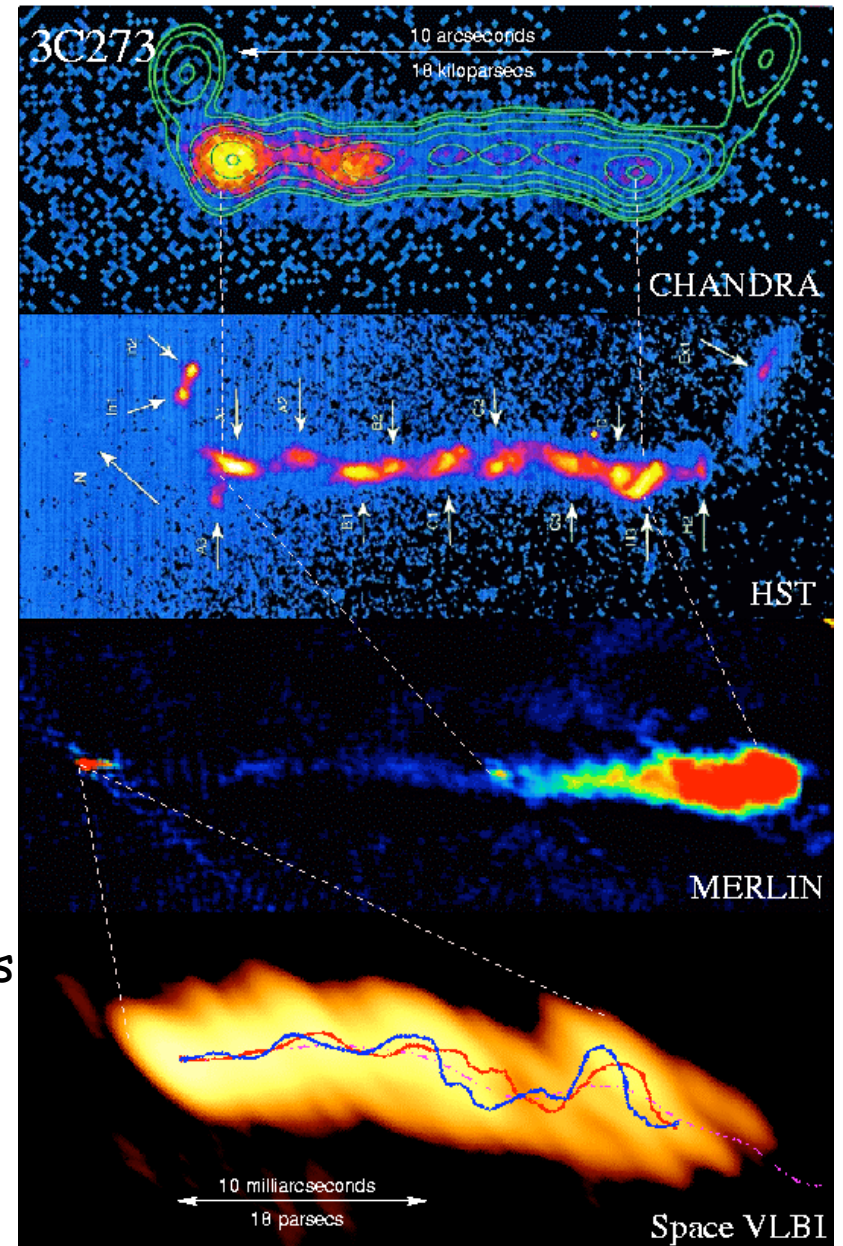
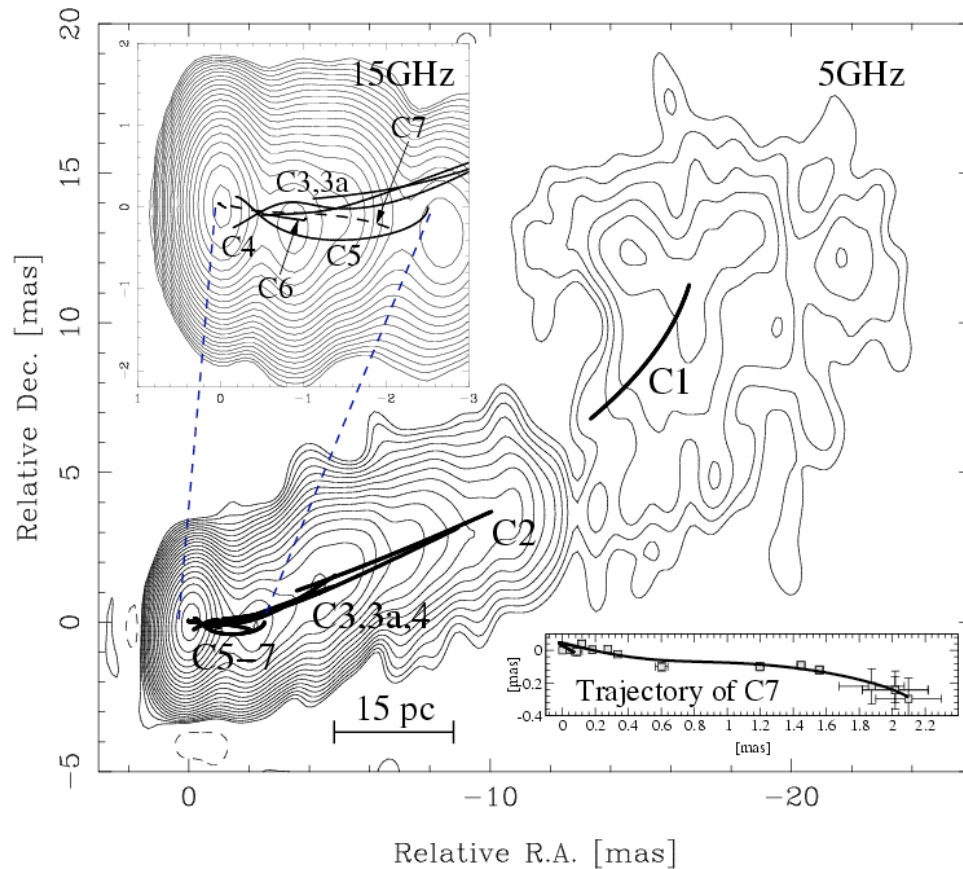
However, lack of bulk-Compton features in soft-X-ray spectra of blazars (**Begelman & Sikora 87, Sikora+97, Sikora & Madejski 00, Celotti+07**) indicates that (1) jets cannot be fully formed (i.e., accelerated to $\Gamma \sim 10$) too close to the center, and (2) cold electrons cannot carry bulk of the jet power.

Kataoka+08: parameters of blazar PKS 1510-089

$$\Gamma \sim 20, r \sim 1 \text{ pc}, R \sim 10^{16} \text{ cm}, N_e/N_p \sim 10, B \sim 0.6 \text{ G}$$

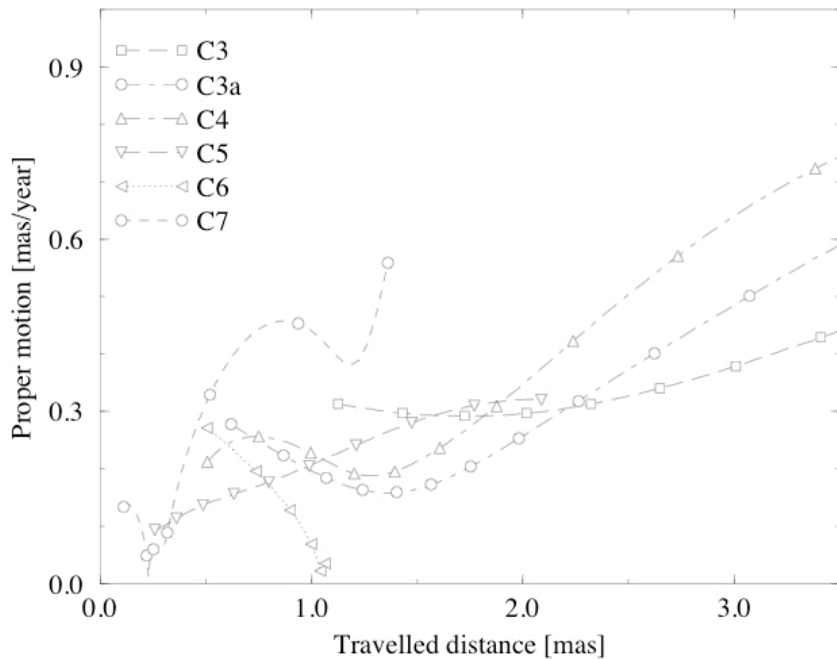
$$L_p \sim 2 \times 10^{46} \text{ erg/s}, L_e \sim 0.1 \times 10^{46} \text{ erg/s}, L_B \sim 0.6 \times 10^{46} \text{ erg/s}$$

Helical VLBI Jets?



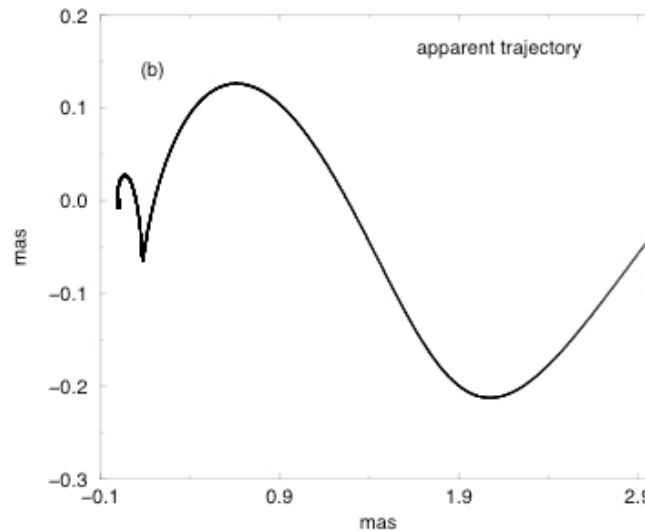
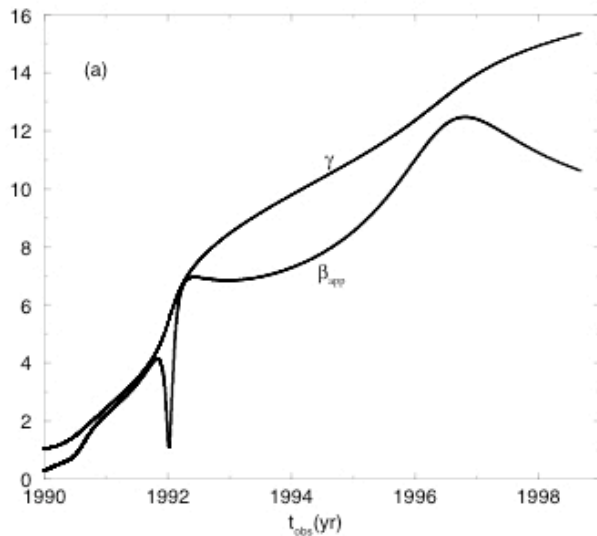
Lobanov & Zensus 01, Lobanov & Roland 05:
 "helical" trajectories of VLBI blobs on pc-scales
 in 3C 345 and 3C 273. If true, may be due to
 the dominant helical MF, but may also reflect
 Kelvin-Helmholtz instabilities in matter-
 dominated jets (Hardee 07, Perucho+07).

Accelerating VLBI Jets?



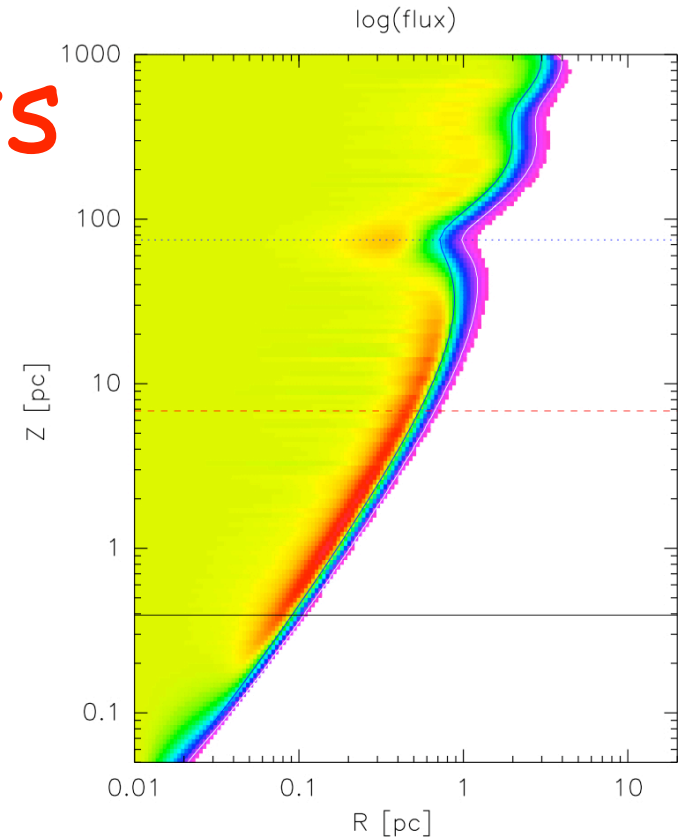
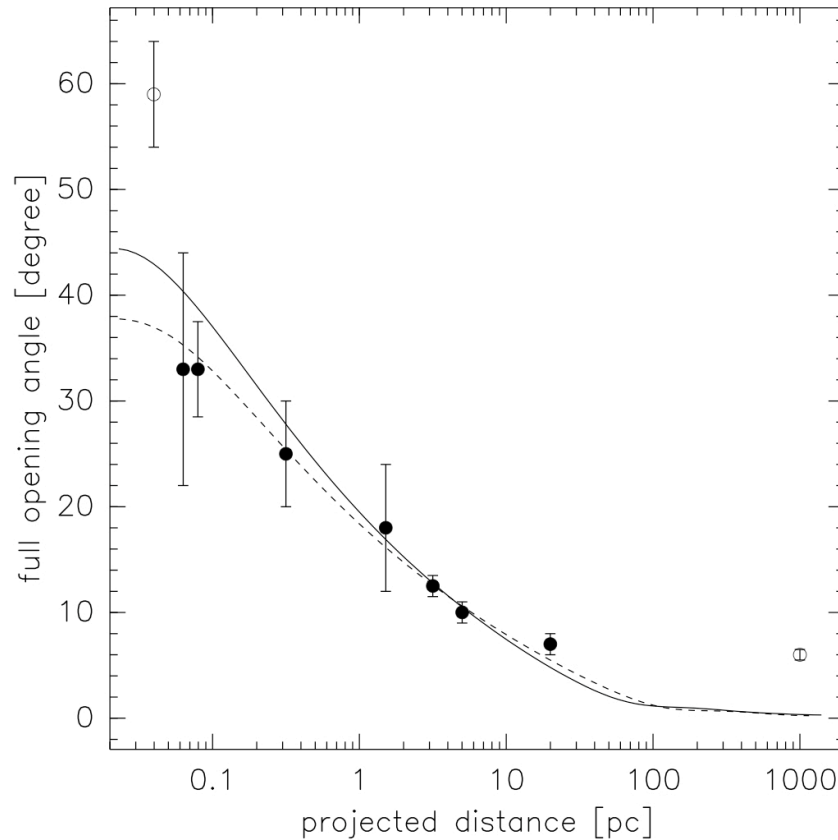
Unwin+97, Lobanov & Zensus 99, Cotton+99, Homan+01, Piner+03: in some cases gradual acceleration of VLBI blobs on $>pc$ scales is observed. However, is it the same blob observed, or different blobs at different distances from the center? Other objects show variety of blobs' apparent velocities, from super- to sub-luminal, including stationary features (Jorstad+01, Cohen+07).

Lobanov & Roland 05: 3C 345



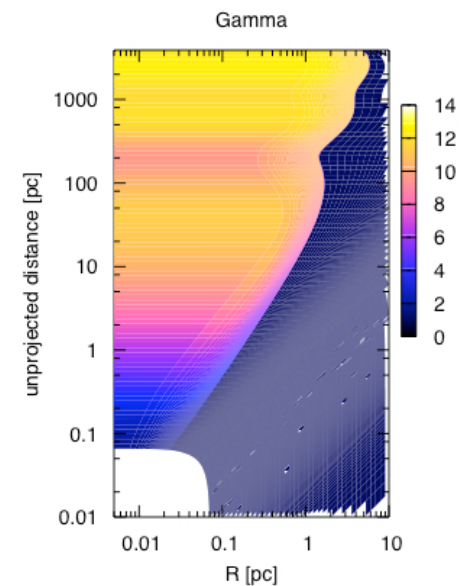
Should we expect magnetic acceleration at work at such large distances from the core, corresponding to $>10^5 r_g$?

Slowly Collimating Jets



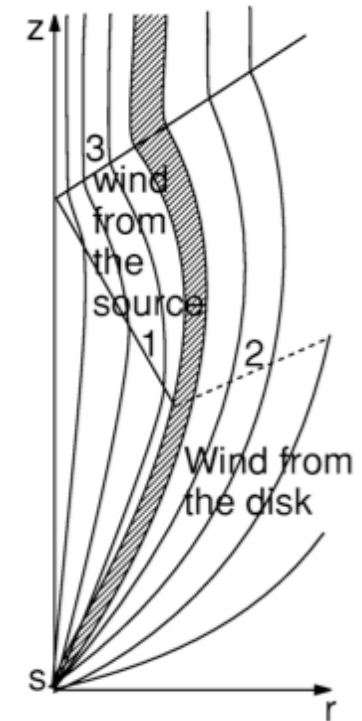
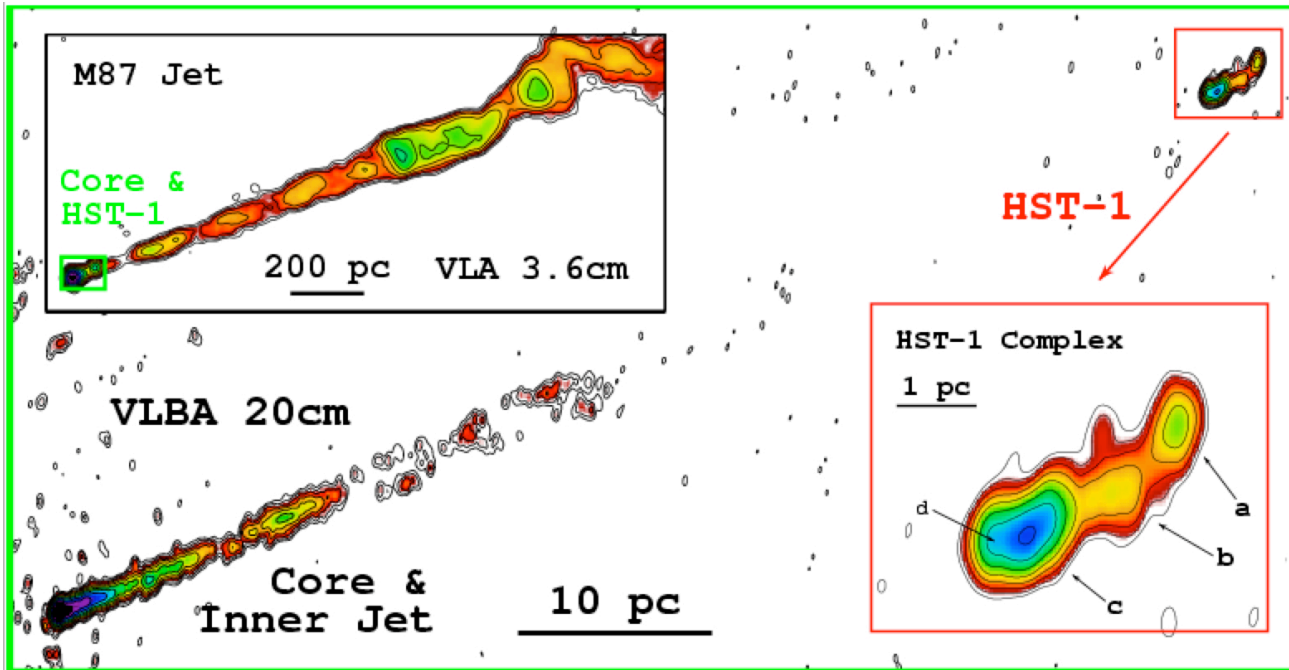
Gracia+05, 08: A two-component model by Bogovalov & Tsinganos provides very good fits to the observed gradual change of the jet opening angle along M87 jet up to 100 pc distances from the center. In addition, radio flux profiles (both along and across the jet) may be explained as well.

However, some other models can explain these data as well!
See, e.g., **Zakamska+08.**



"Recollimation" Nozzle

Cheung+07: multiscale M87 jet



In a two-component model by Bogovalov & Tsinganos, recollimation shock is always present. When applied to M87 jet (Gracia+08), position of this feature agrees with the location of the HST-1 knot. Broad-band variable emission of this knot may be indeed understood as being produced in a compact nozzle formed by a converging shock (Cheung+07).

However, hydromagnetic model of the jet may qualitatively reproduce position of the HST-1 knot/reconfinement nozzle as well (Stawarz+06).

Polarization of pc-Scale Jets

- Radio-to-optical polarization of blazars indicate typically B_{\perp} for the unresolved cores (especially in the case of BL Lacs), and variety of configurations for the resolved sub-pc scale jets (Impey+91, Cawthorne+93, Gabuzda & Sotho 94, Cawthorne & Gabuzda 96, Stevens+96, Nartallo+98, Gabuzda+00, Lister & Homan 05, Jorstad+07).
- B_{\perp} may indicate compression of the tangled magnetic field by shocks, while B_{\parallel} shearing of the tangled magnetic field due to velocity gradients (Laing 80, 81, Hugh+89). This would be consistent with matter-dominated outflows.
- B_{\perp} could also be due to the dominant toroidal MF. Such interpretation is consistent with B_{\perp} observed at the spatially extended regions where the jets bend, and also with the observed altering B_{\perp} - B_{\parallel} structures (Gabuzda+04).
- Interpretation of the blazar polarization data is complicated and in some cases not conclusive due to the relativistic effects involved (Lyutikov+05; ask Mitch Begelman and Robert Laing for details).

Spine-Shear Layer Structure

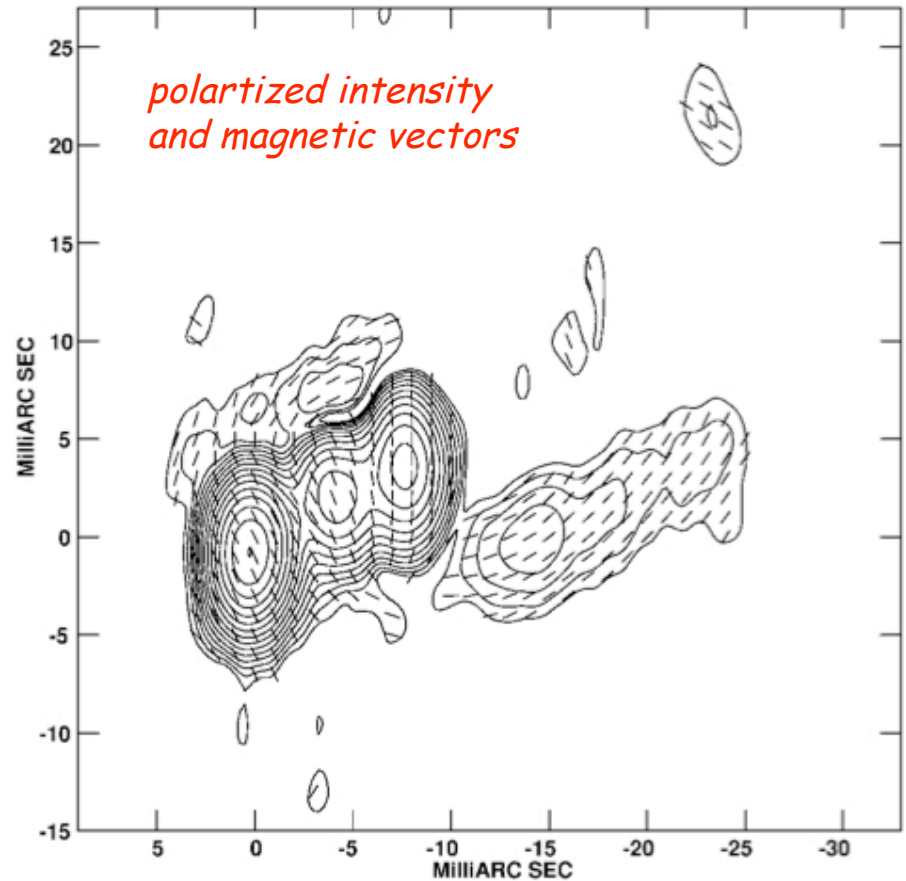
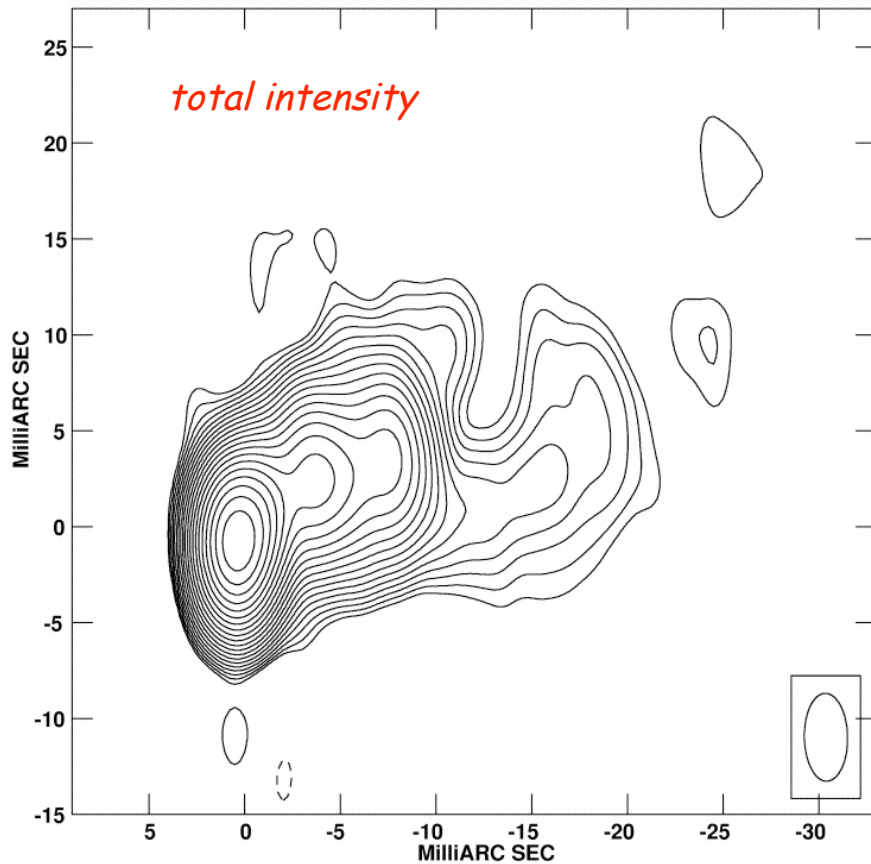


FIG. 1b

Attridge+99: Spine B_{\perp} / boundary layer B_{\parallel} structure in 1055+018.
Shock compression/velocity shear in the matter-dominated jet,
or helical MF in the current-carrying outflow?
(Similar cases: Gabuzda+01, Pushkarev+05)

RM Gradients: Expected

$$c^2 k^2 = \zeta \omega^2$$

$$\zeta = 1 - \frac{\omega_{\text{pl}}^2}{\omega(\omega \pm \omega_L)}$$

$$v_{\text{ph}} = \frac{\omega}{k}, \quad v_{\text{gr}} = \frac{\partial \omega}{\partial k}$$

$$\Delta\chi = \frac{2\pi e^3}{m_e^2 c^2 \omega^2} \int_0^L n_{\text{th}} B_{0,\parallel} ds$$

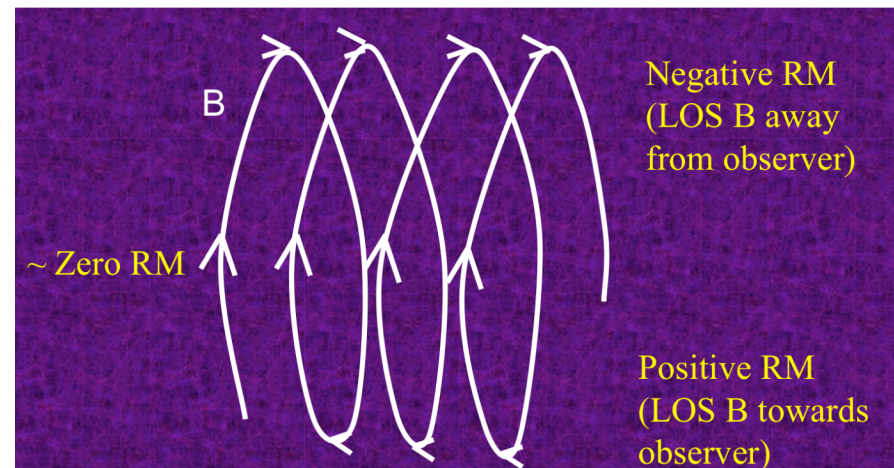
$$\left(\frac{\Delta\chi}{\text{rad}}\right) = RM \cdot \left(\frac{\lambda}{\text{m}}\right)^2$$

$$RM = 0.81 \int_0^L \left(\frac{n_{\text{th}}}{\text{cm}^{-3}}\right) \left(\frac{B_{0,\parallel}}{\mu\text{G}}\right) \left(\frac{ds}{\text{pc}}\right)$$

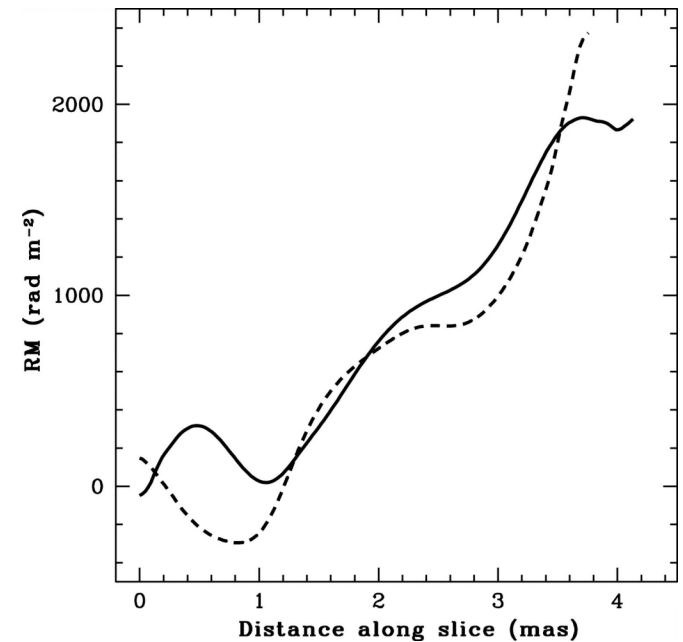
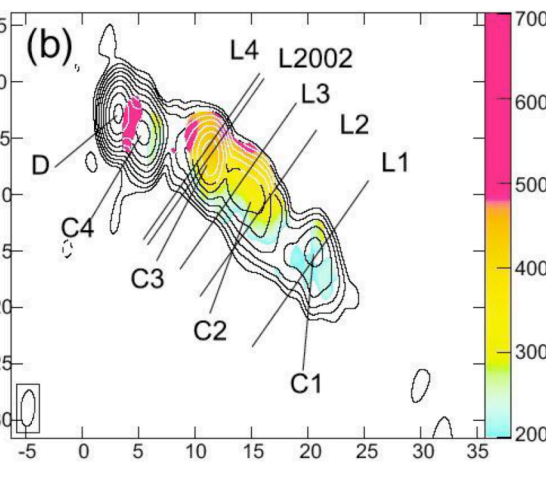
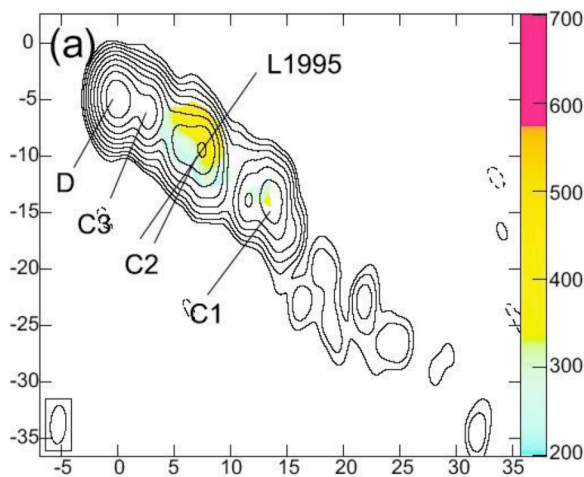
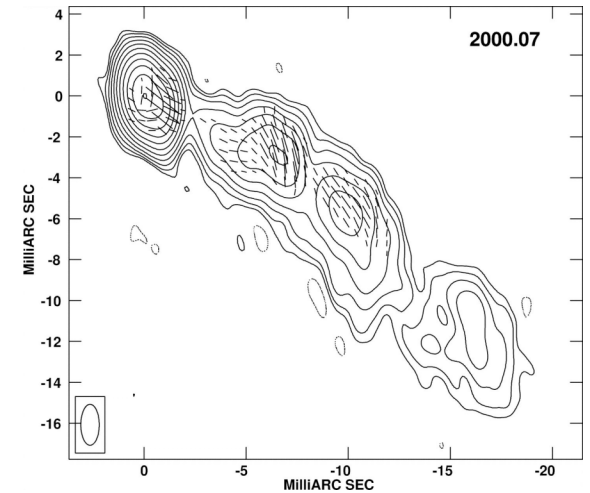
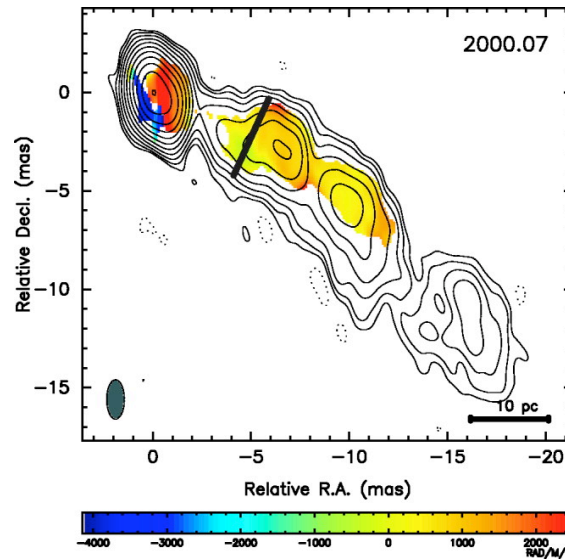
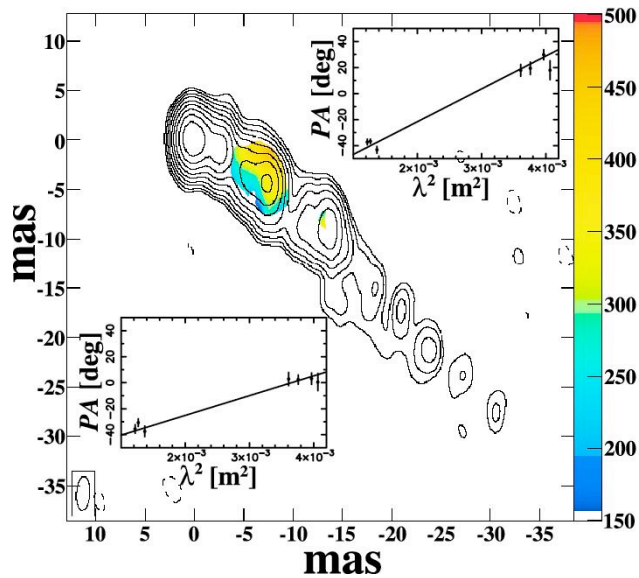
RM gradients across a jet should be expected in the case of a helical magnetic field (Blandford 93)

When propagating through a magnetized plasma ("external screen"), a polarized wave experiences rotation of a plane of polarization. That is because any plane polarized wave can be treated as a linear superposition of a right-hand and left-hand circularly polarized component. Circularly polarized wave with positive helicity has different phase velocity than the wave with negative helicity within the magnetized environment.

Gabuzda 06



RM Gradients: Observed, Variable



3C 273: Asada+02, 08, Zavala & Taylor 05
 (other examples: Gabuzda+04)

Where Is Faraday Screen?

Faraday screen has to be external to the emitting region because:

- Rotations $>45\text{deg}$ sometimes observed (Sikora+05).
- RM gradients sometimes localized where the jet interacts with the clouds of ISM (3C 120; Gomez+00, 08).
- λ^2 dependence always holds.
- Decrease of RM along the jets observed (Zavala & Taylor 02, 03, 04).
- High fractional polarization observed from the RM gradient regions.

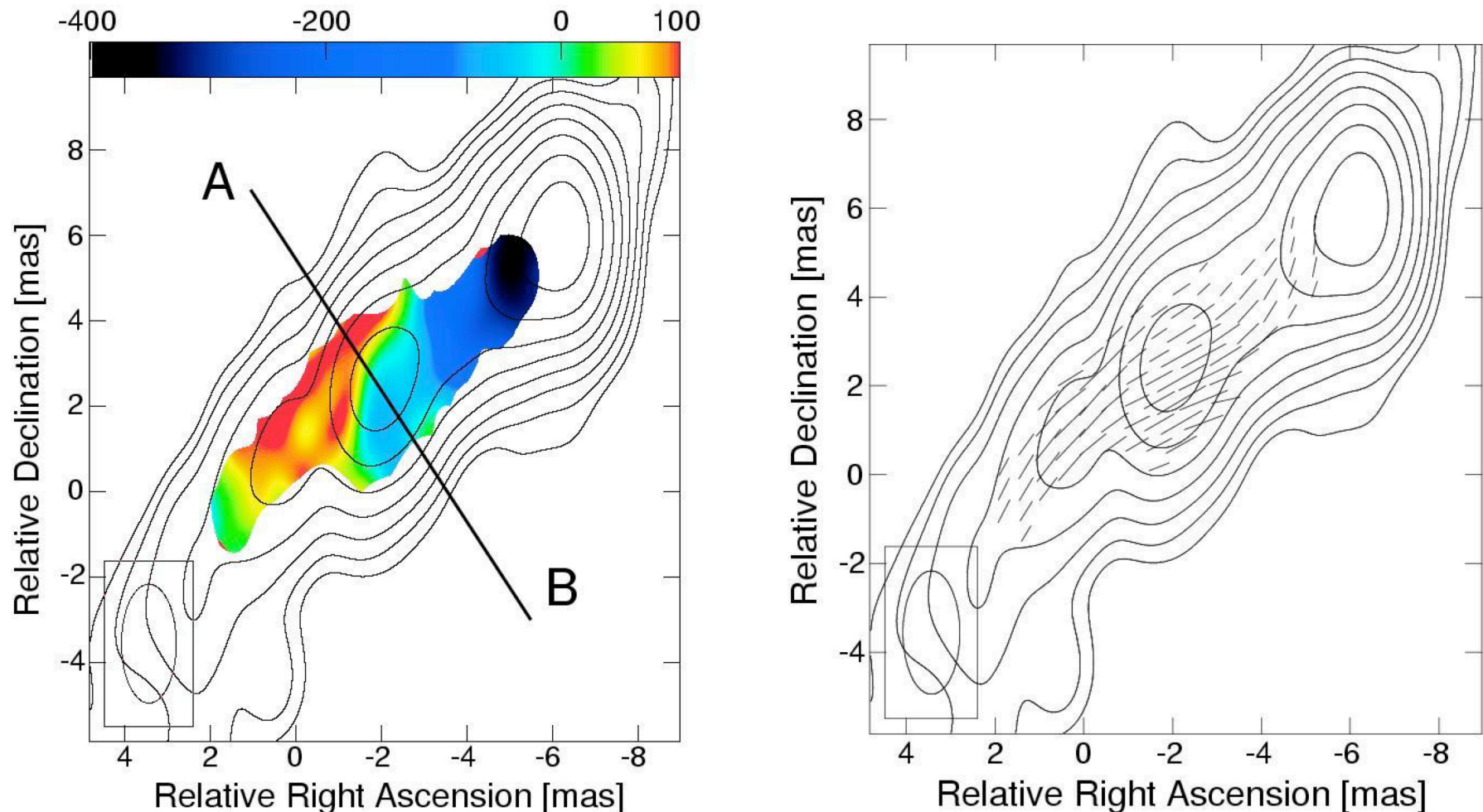
Faraday screen cannot be completely unrelated to jet because:

- RM gradients vary on timescale of years (Zavala & Taylor 05, Asada+05).
- Direction of RM gradients always agrees with a sign of a circular polarization observed (Gabuzda+08)*.

Spine/Sheath structure again?

**CP may result from Faraday conversion of LP mediated by helical MF. The sign of CP is then determined by the helicity of MF, and so should agree with the direction of the RM gradient.*

The case of NRAO 140



Asada+08: **B** || polarization structure in NRAO 140 together with strong RM gradient suggest loosely wound magnetic helix in a jet spine (where most of the radio emission is produced), and tightly wound magnetic helix in an outer sheath (which acts as a Faraday Screen).

Small (sub-kpc) Scales - Summary

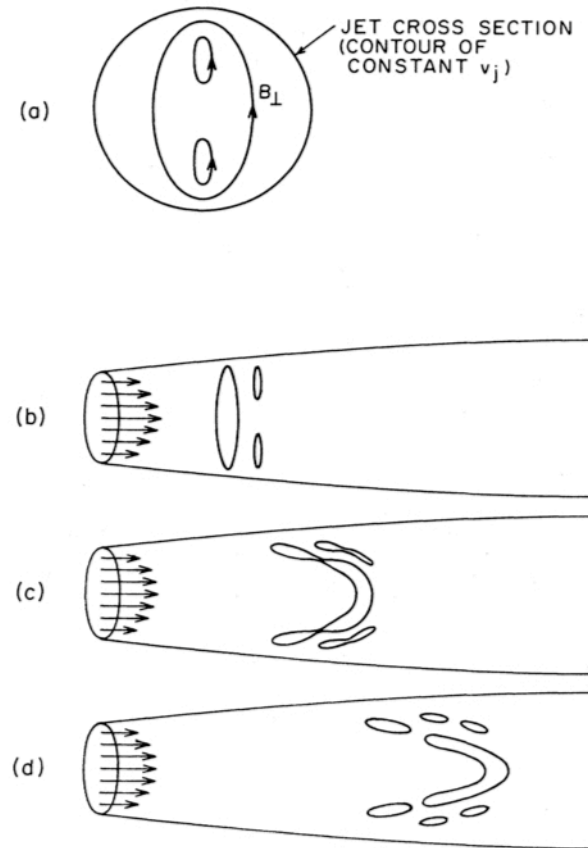
- Standard modeling of blazars (shock acceleration, leptonic emission) indicates matter (proton!)-dominated jets on $0.1-1 \text{ pc} \sim 10^3-10^4 r_g$ scales. If correct, this would be consistent with the conversion of Poynting-dominated outflow to mass-loaded kinetic-dominated one due to, e.g., kink instabilities (**Sikora+05**).
- Several observational findings are however consistent with the dynamical domination of a toroidal (\neq helical) MF on much larger distances of $1-100 \text{ pc} \sim 10^4-10^6 r_g$. Some of these findings should be still taken with caution (helical trajectories, acceleration of blobs). Some other seem to be on the other hand more robust (RM gradients, slow collimation of jets). These point to the multi-component jet structure.
- The most recent observations of extremely rapid (200s) variability of blazars at TeV energies (PKS 2155; **Aharonian+07**, **Begelman+07**), as well as spectacular broad-band (blazar-like) outburst of the HST-1 knot in M87 jet (**Harris+06**, **Cheung+07**) may suggest that "standard blazar models" have to be critically re-examined (see in this context **Marscher+08**).

Kpc-Mpc Scales

- In the case of a matter-dominated jet, when the MF is frozen-in to the fluid, one expects $B_T \propto r^{-1}$ and $B_p \propto r^{-2}$ (conservation of MF energy flux and MF flux; **Begelman+84**). Thus, the toroidal MF should dominate over the poloidal one on large scales. This simple scaling is roughly consistent with the equipartition MF intensity:

$$B_{eq} \sim B \sim B_{blaz} (pc/100kpc) \sim B_E (r_g/100kpc) \sim 1-10\mu G$$

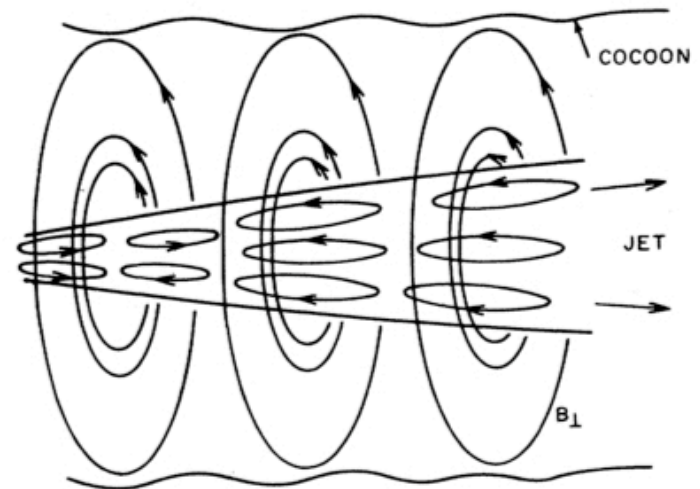
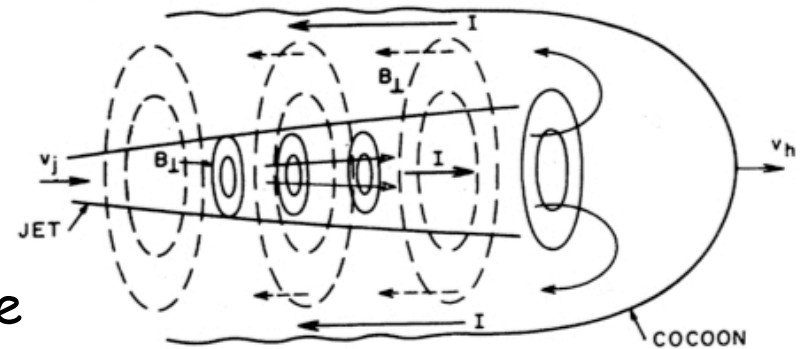
- However, polarimetry of large-scale jets in powerful quasars and radio galaxies indicate $B_{||}$. This may suggest action of a velocity shear (re-)orienting MF lines (**Laing 80, 81**). The regions with strong velocity shear are likely to be the sites of the enhanced magnetic reconnection, dynamo action, and injection of turbulence, and therefore of the enhanced particle acceleration/energy dissipation (**De Young 86**).
- Note that the longitudinal MF component cannot be unidirectional on large scales, since this would imply too large magnetic flux: $B_{eq} (kpc)^2 \gg B_E r_g^2$. Thus, $B_{||}$ must indeed reverse many times across the jet (**Begelman+84**).



Begelman+84

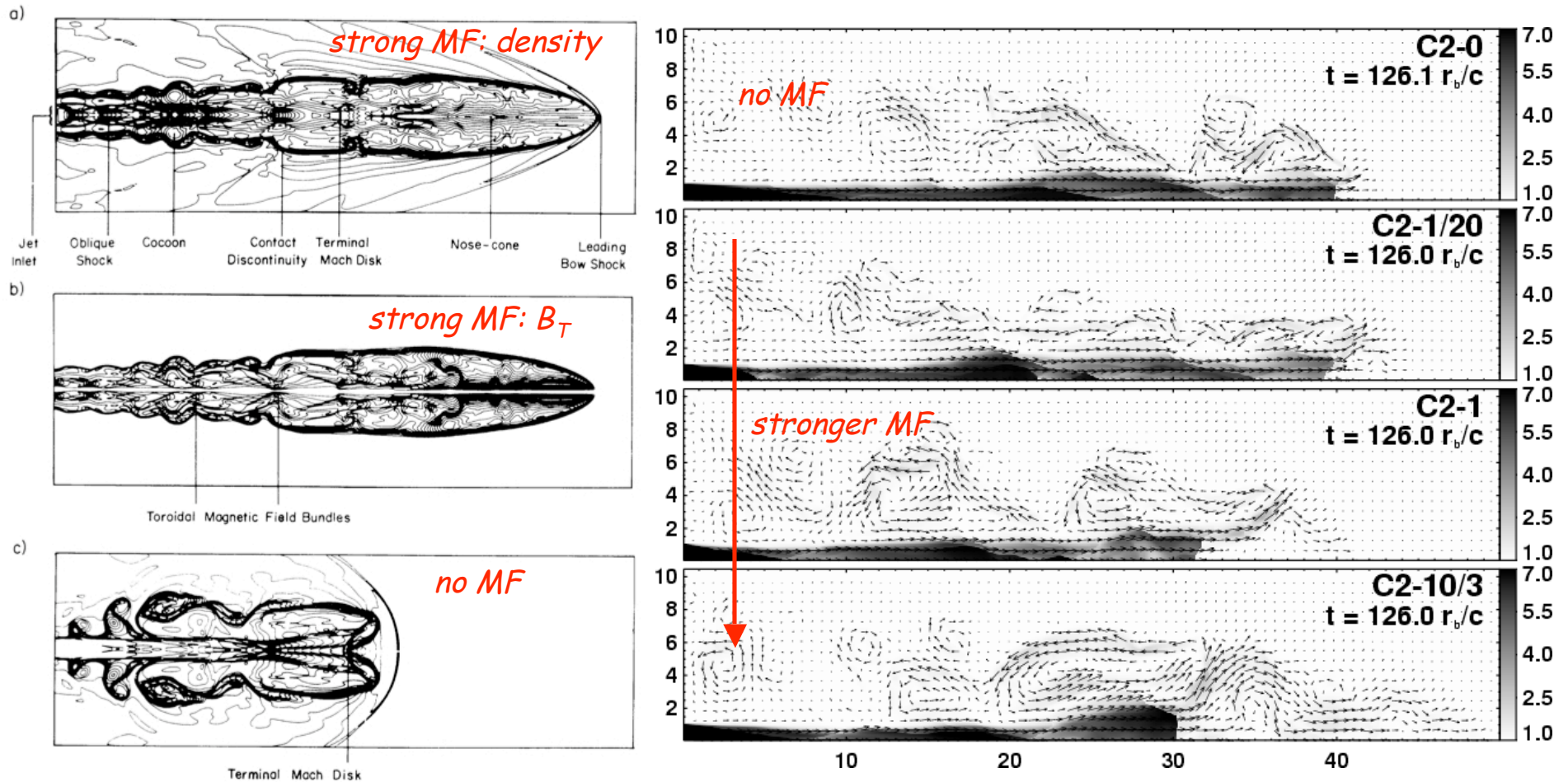
Jet Confinement

- Jets with toroidal MF can be self-confined due to magnetic tension involved: $B_T^2/4\pi = p_j$ (Benford78, Chan & Henriksen 80, Bicknell & Henriksen 80, Bridle+81).
- Toroidal MF implies a net current flowing along the jet, $B_T \sim 2I/cR_j$. If the ambient medium behaves as a perfect conductor, the return current is induced on the interface between the cocoon and the ambient medium (or throughout the cocoon, and/or on the surface of the jet), such that $p_{ext} \sim p_j (R_j/R_{ret})^2$ (highly overpressured jets, underpressured cocoons!).
- If shear effects are important, the force-free equilibrium may establish: magnetic tension (B_T) confines highly overpressured (B_p) jet spine.



Begelman+84

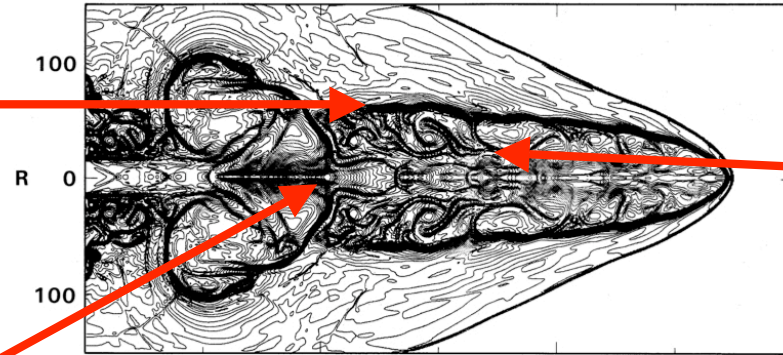
Large-Scale Morphology



Clarke+86, Lind+89, Kossel+90, Komissarov 99, Leismann+05: 2D axisymmetric ideal MHD simulations of strongly magnetized jets (with no substantial poloidal MF) reveal thin ("no-backflow") cocoons and "nose-cone" morphology of jet termination regions (different from hydro jets!).

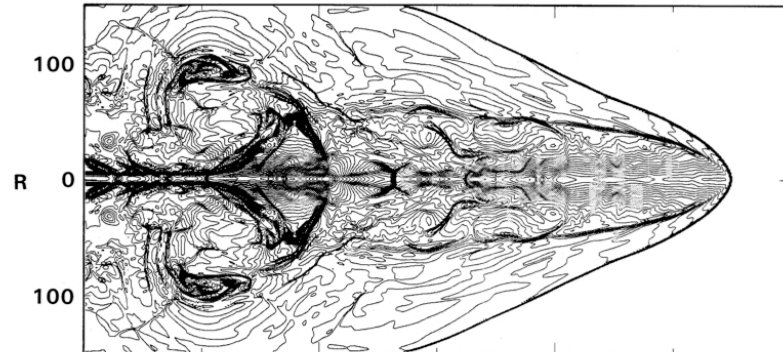
Nose-Cone Structures

Contact discontinuity: here the return current flows (in the case of an ideal MHD).



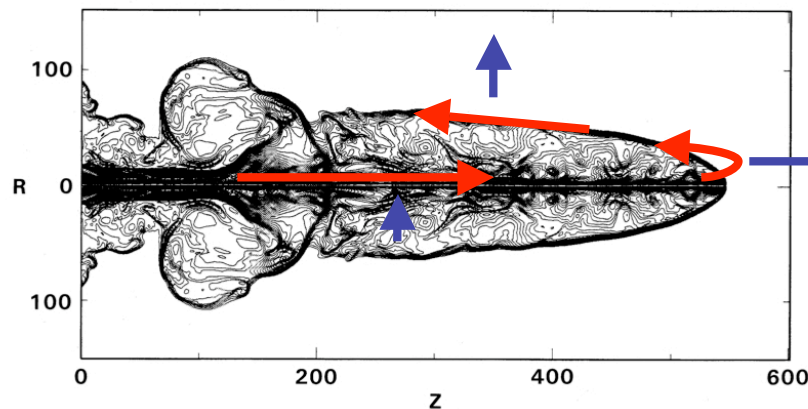
"Nose": here the current-carrying plasma is confined by the self-induced toroidal MF which also prevents any backflow.

Mach disk: here most of the fluid kinetic power is thermalized.



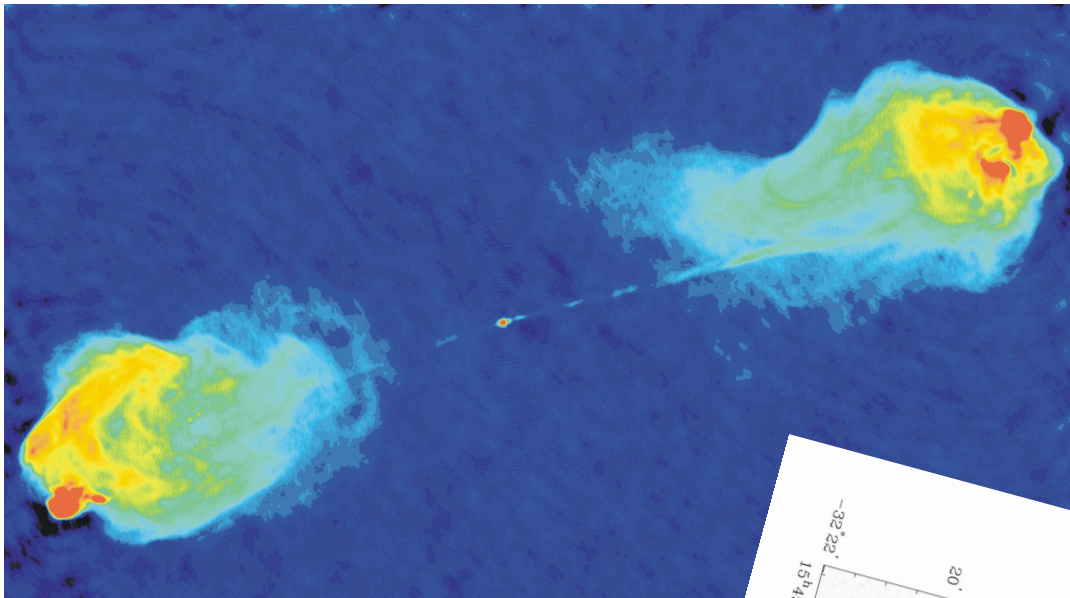
The Lorentz force $\mathbf{j} \times \mathbf{B}_T$ pinches (collimates) the jet, drives expansion of the jet head, and drives expansion of the cocoon.

Is it consistent with observations?
Is it not an artifact of the 2D axisymmetric simulations? (no reconnection!)

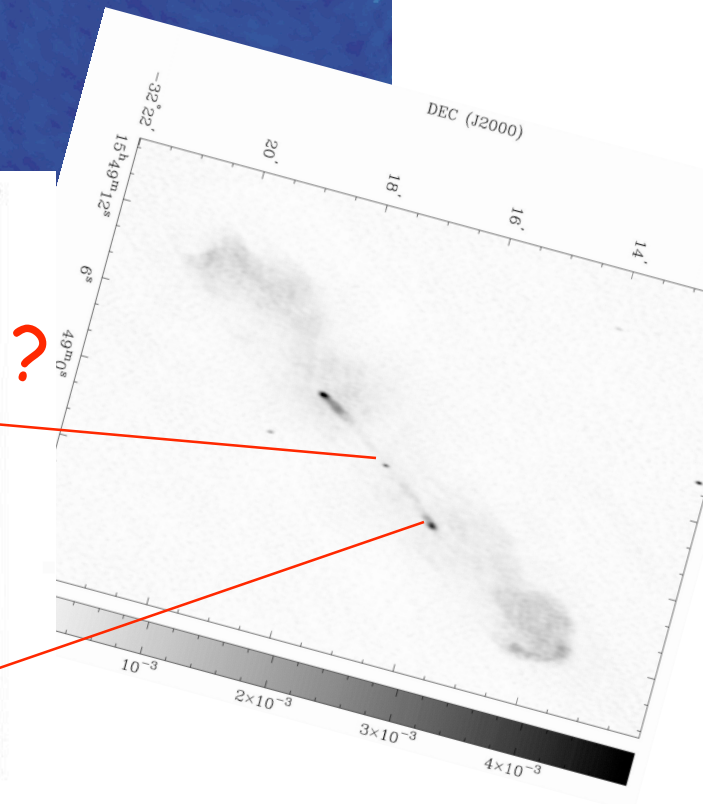
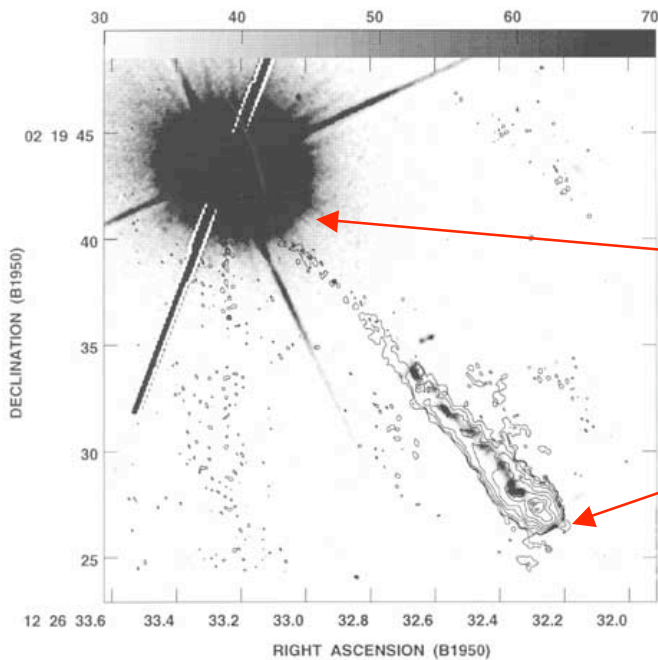


Lind+89: matter density, gas pressure, magnetic field

FR II Radio Galaxies

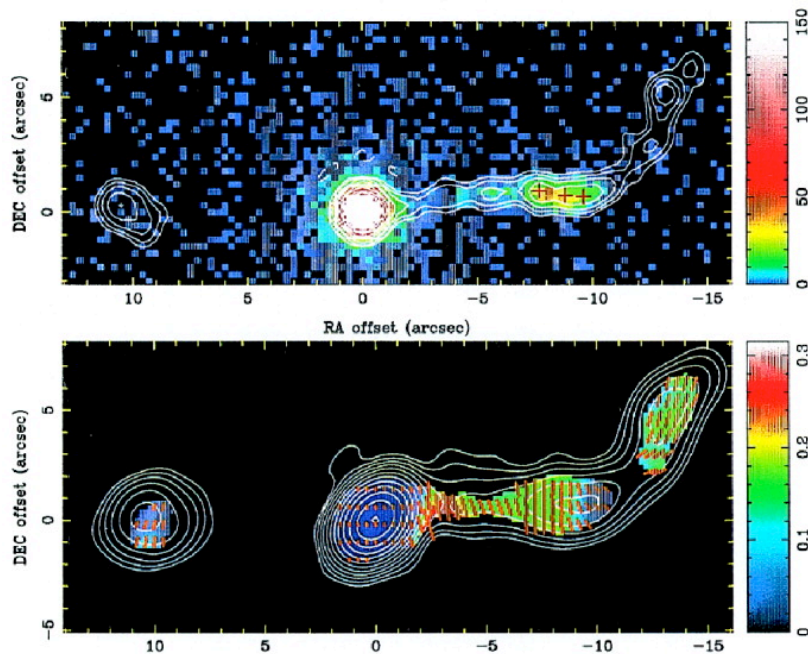


Classical FR II morphology (e.g., Cygnus A; Carilli & Barthel 96) is consistent with matter-dominated jet (fat lobes, no nose-cones, substantial backflows).



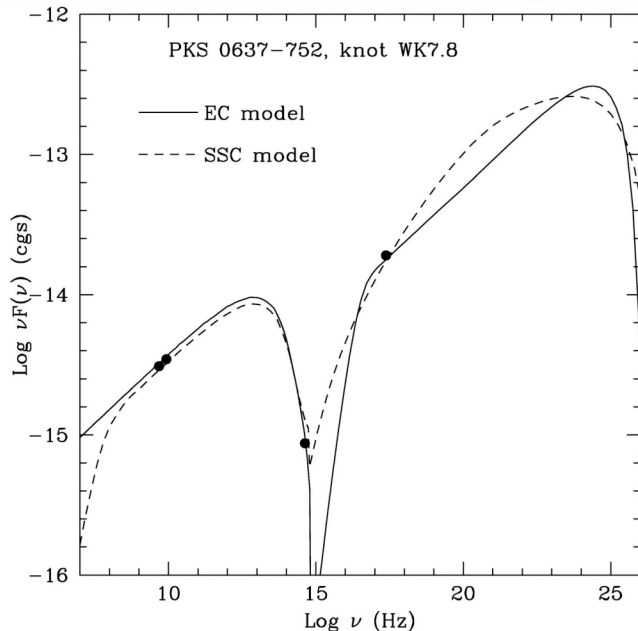
"Problematic" cases of one-sided jets/lobes with narrow cocoons (e.g., 3C 273, Bahcall+95) can be explained as inner structures of double-double radio sources (e.g., PKS B 1545; Saripalli+03), without invoking strong MF (Stawarz 04).

Chandra Quasar Jets



Chandra X-ray Observatory detected surprisingly intense X-ray emission from large-scale (100 kpc - 1 Mpc) quasar jets ($L_X \sim 10^{44}-10^{45}$ erg/s). Many examples (e.g., Schwartz+00, Cheung+, Hardcastle+, Harris+, Jorstad+, Kataoka+, Kraft+, Marshall+, Sambruna+, Siemiginowska+).

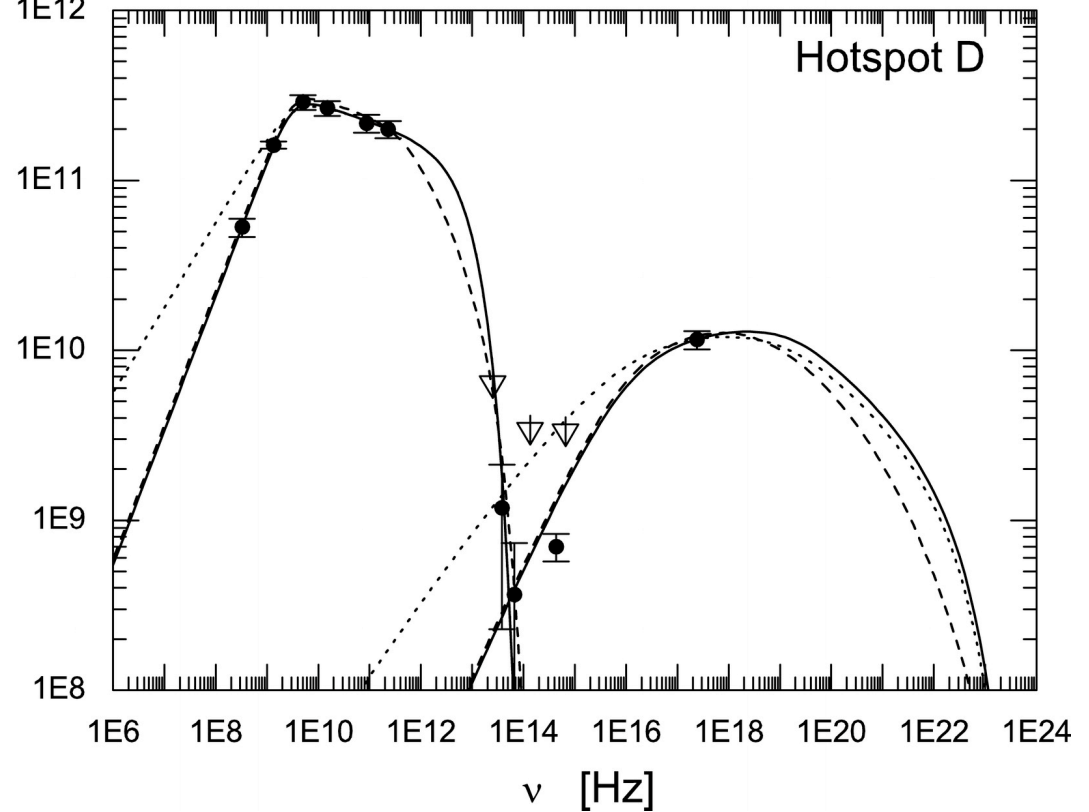
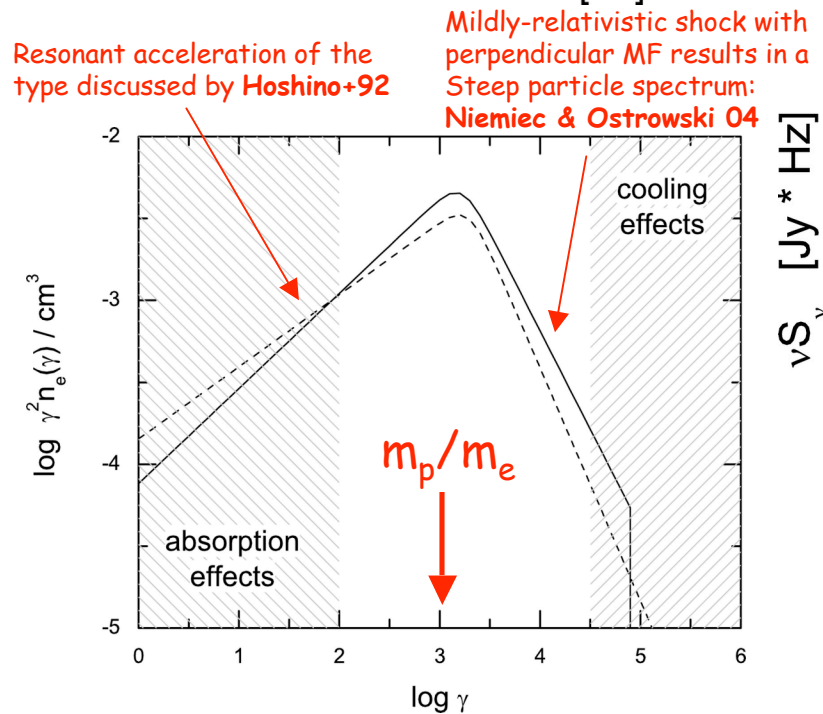
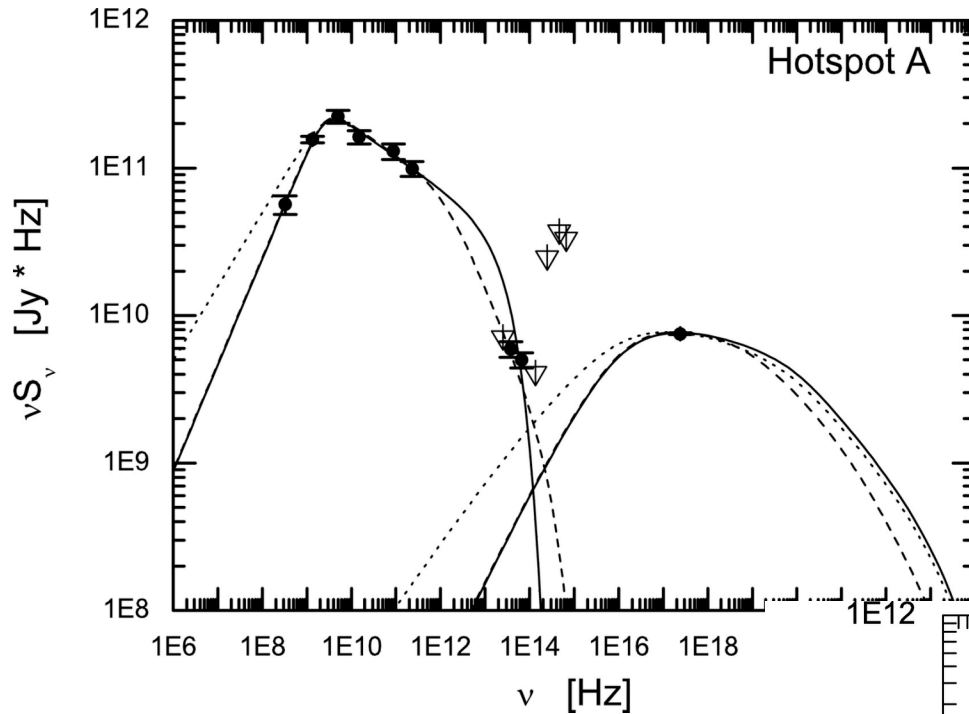
It was proposed that this X-ray emission is due to inverse-Compton scattering of the CMB photons by low-energy jet electrons, $E_e \sim 100$ MeV. (Tavecchio+00, Celotti+01).



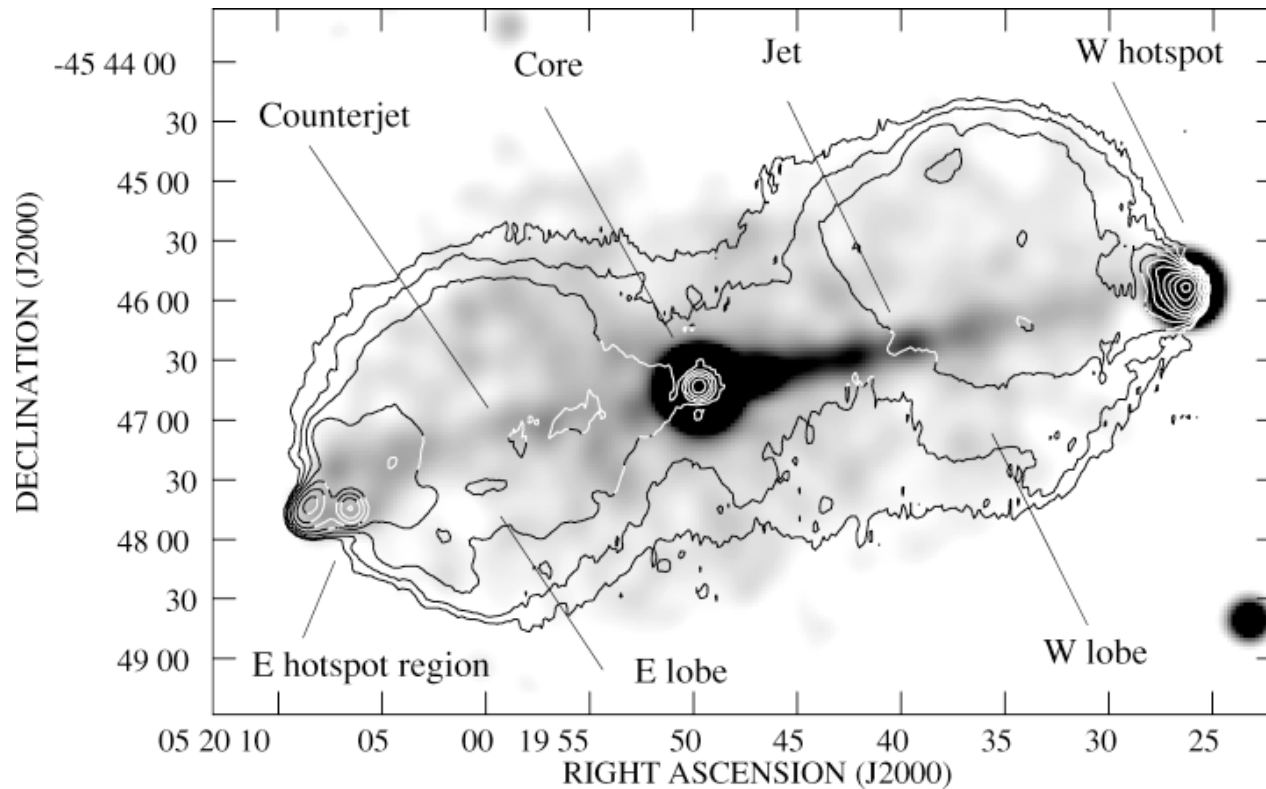
IC/CMB model requires highly relativistic bulk velocities ($\Gamma > 10$) on Mpc scales, and dynamically dominating protons, $L_p > L_e \sim L_B$ with $B \sim B_{eq} \sim 1-10 \mu G$. Note that for $\Gamma < 10$ the IC/CMB model would imply $B \ll B_{eq}$

Hotspots

Stawarz+07: analysis of the broad-band emission of hotspots in the exceptionally bright radio galaxy Cygnus A indicates $U_B \sim U_e$ and terminal shocks dynamically dominated by protons.



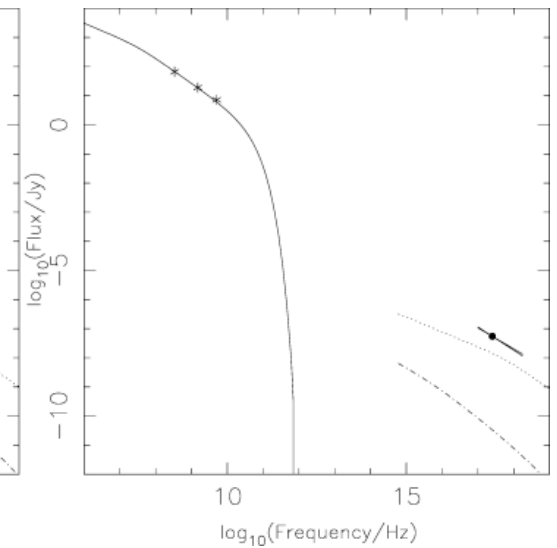
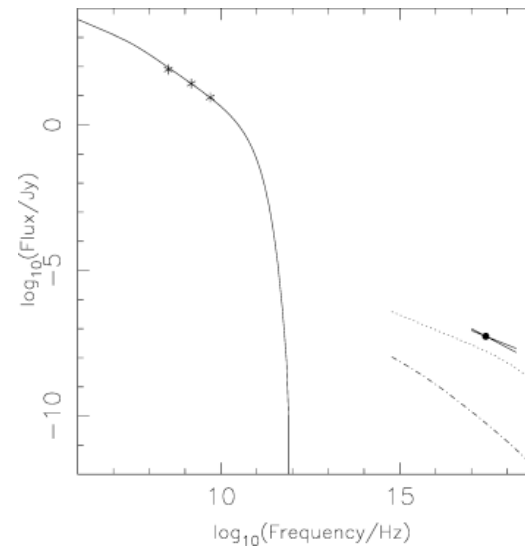
Lobes



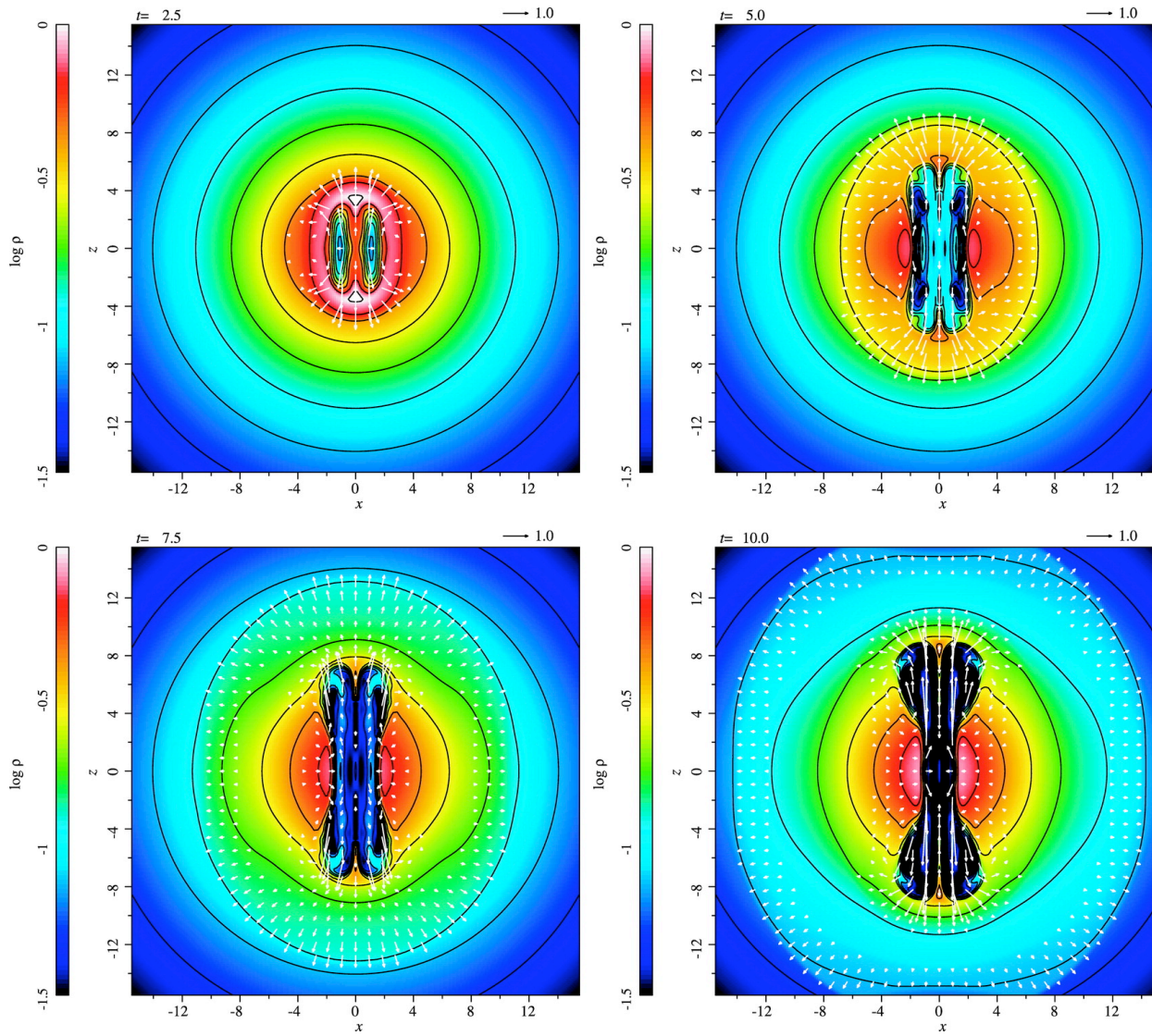
Hardcastle & Croston 05: X-ray and radio emission from the lobes of Pictor A radio galaxy.

X-ray and radio lobe emission in this and many other sources (Croston+05, Kataoka & Stawarz 05) indicates energy/pressure equipartition

$$U_B \sim U_e .$$



"Magnetic Tower" Jets

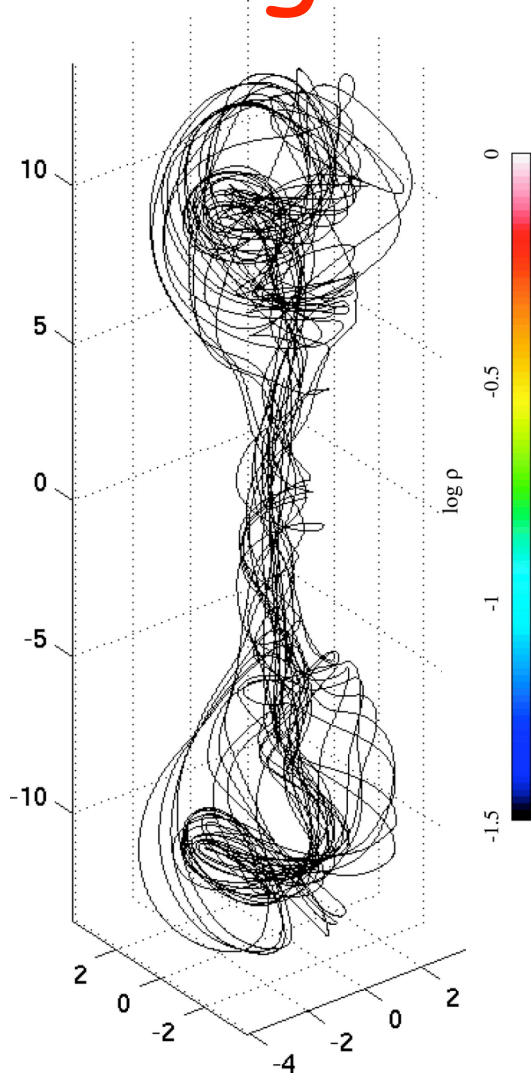


Density (colors) and poloidal velocity field (arrows).

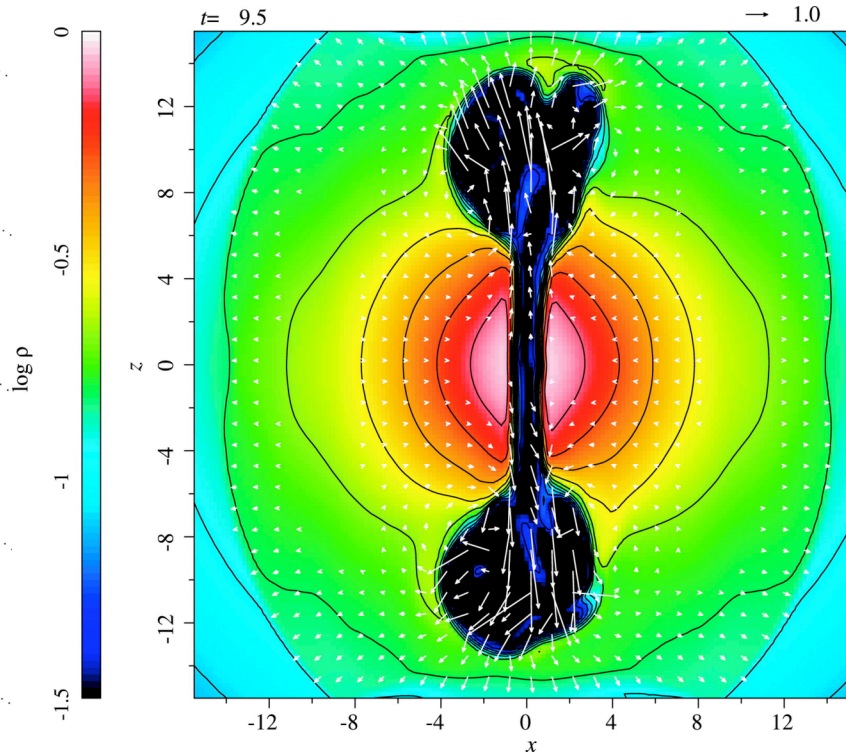
Li+06, Nakamura+06,07,08:
3D ideal MHD simulations of strongly magnetized jet propagating (on large, >10 kpc scales) in a gravitationally stratified gaseous background in hydrostatic equilibrium. The injected Lynden-Bell "magnetic tower" jet is made of a large-scale helical (but not force-free) MF with poloidal flux and poloidal current. Jets and lobes are magnetically dominated.

Magnetic dominance in lobes and global helical MF on large scales seem to contradict the observations of FR I-inflated cavities in clusters (Dunn+06, Birzan+08, Croston+08). The involved leading field over a range disk radii may be too strong.

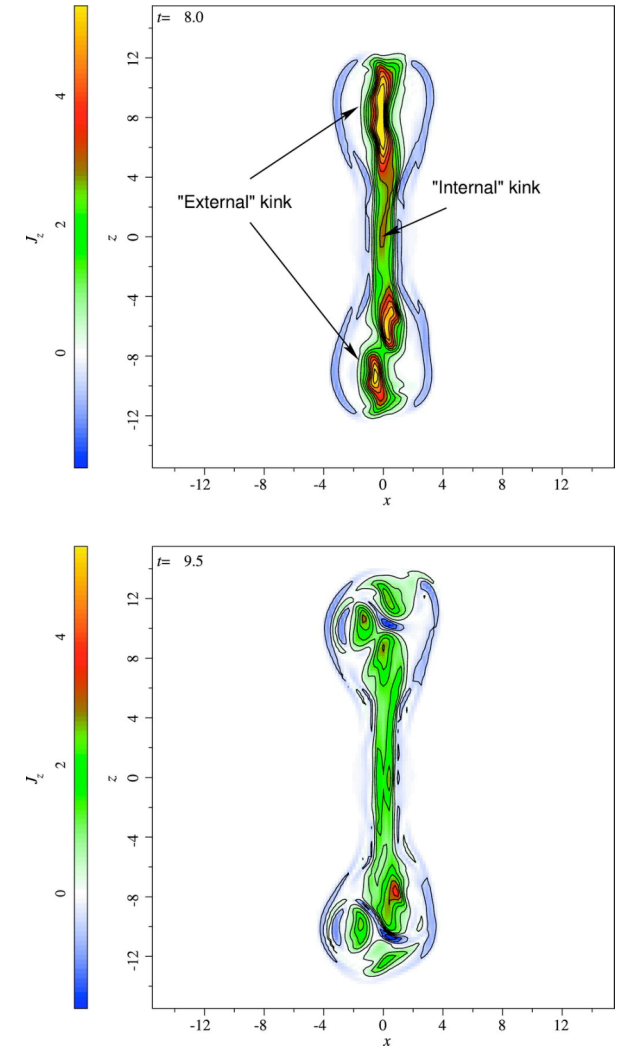
Large-Scale Magnetic Structure



Large-scale MF helix



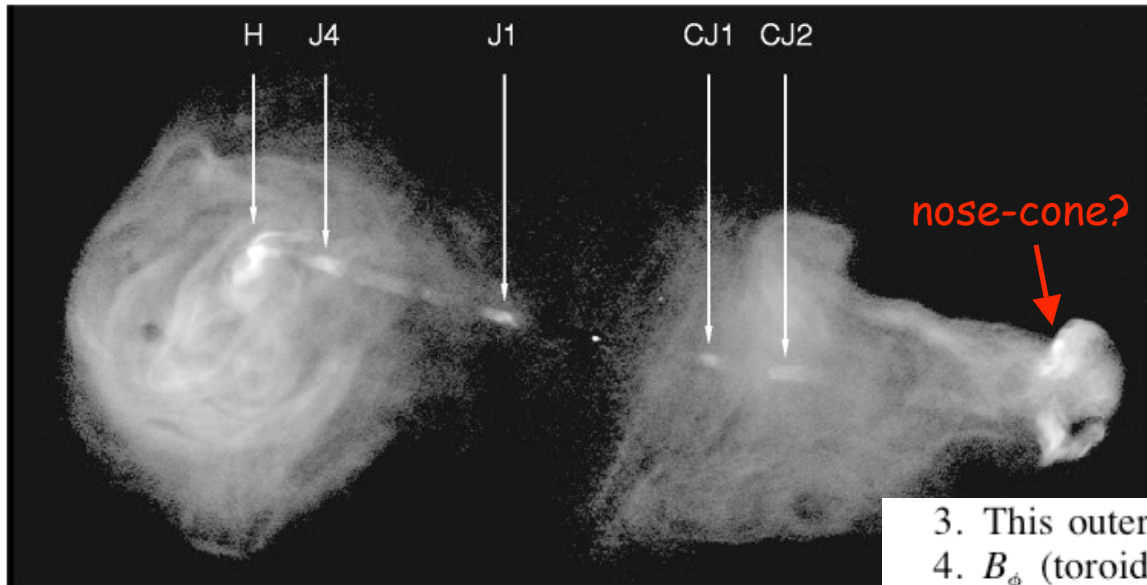
Density and poloidal velocity field



Current distribution and developing kink instabilities

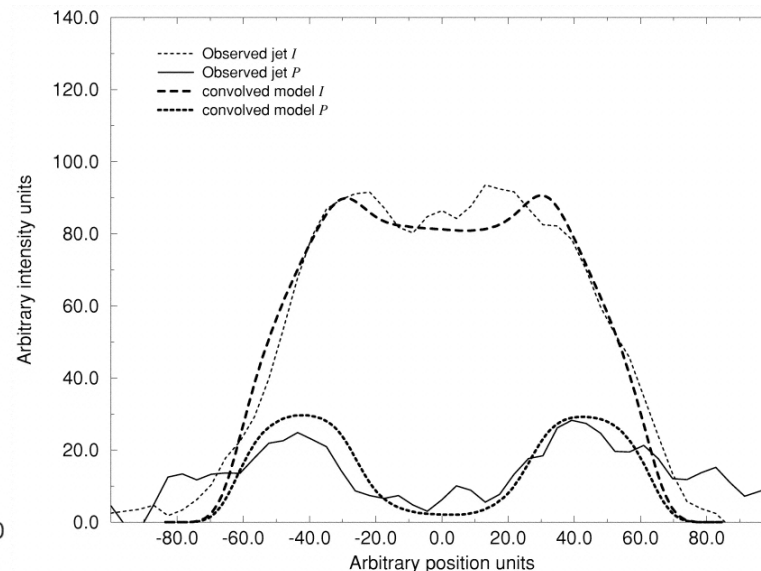
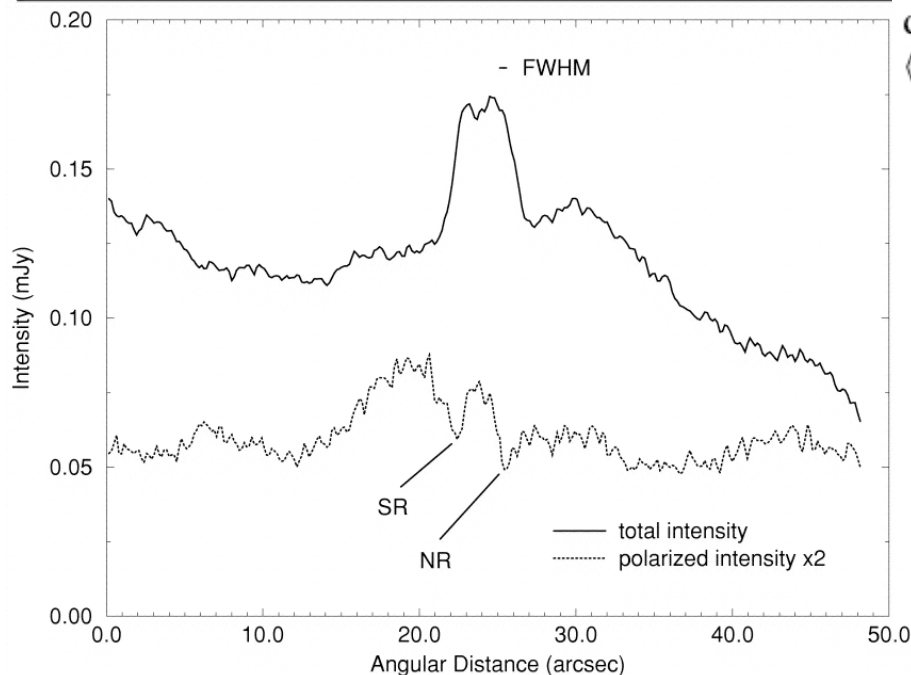
[Li+06](#), [Nakamura+06,07,08](#)

The Case of 3C 353



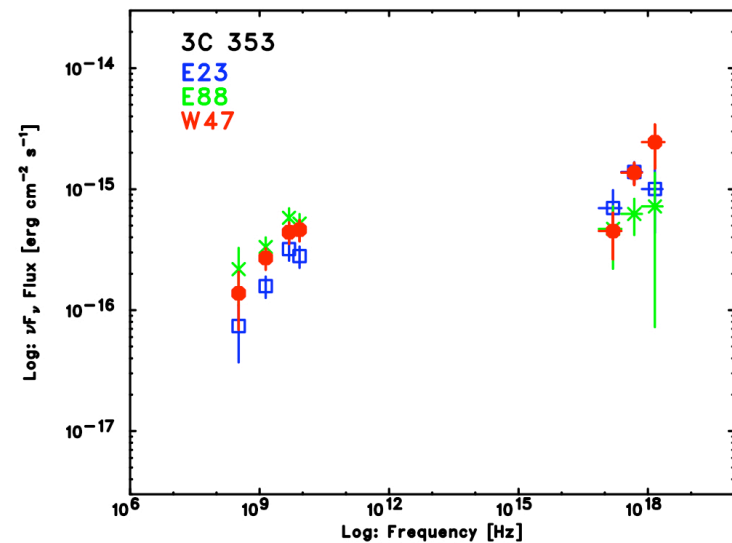
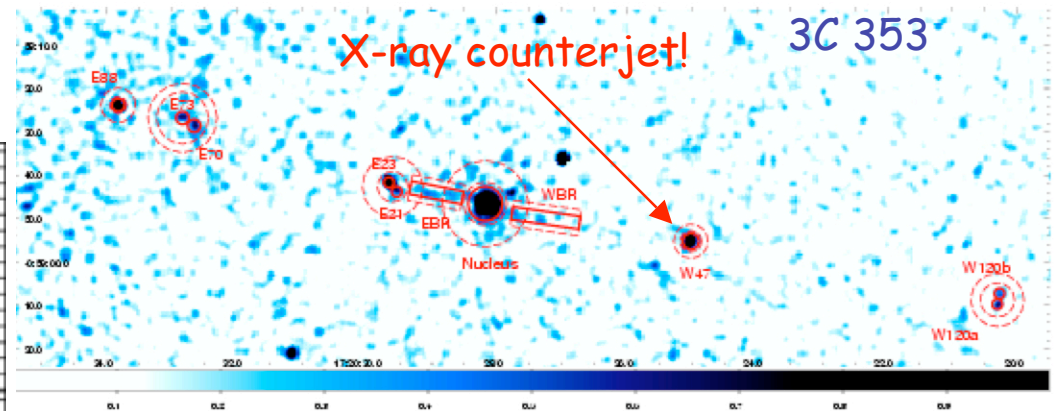
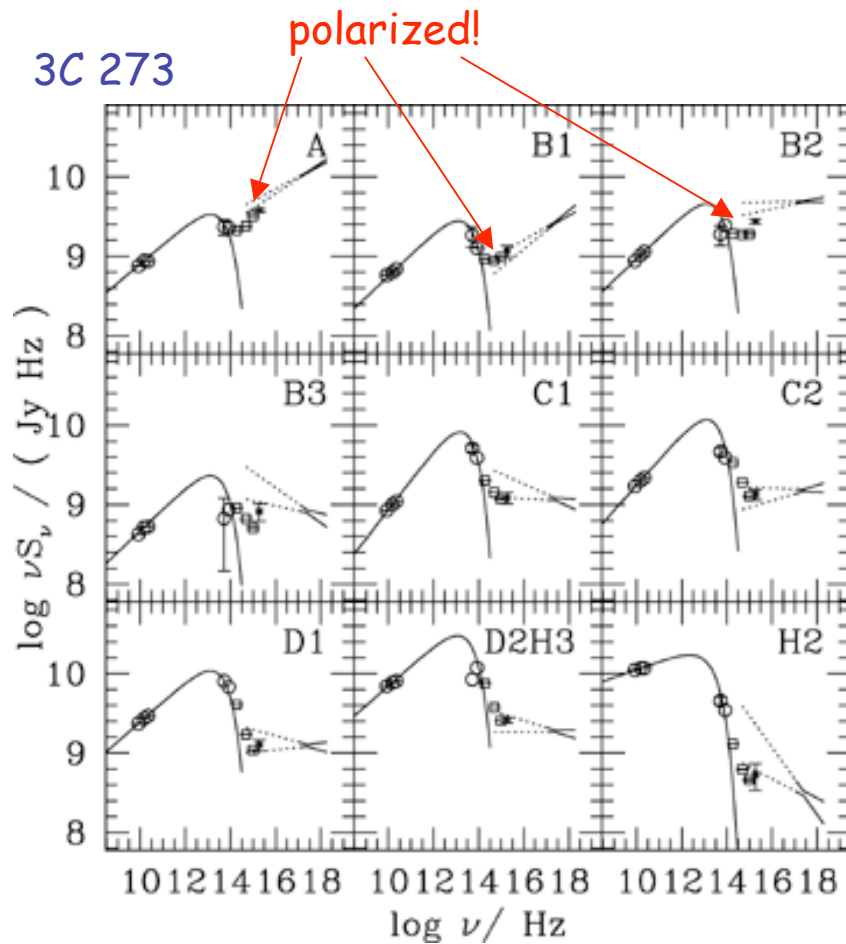
Swain+98: most of the jet radio emission is produced in a boundary layer with apparently parallel MF orientation. Polarization rails along the jets result from vector cancellation of this emission with the orthogonally polarized lobe emission.

3. This outer layer has no radial field component B_r ; and
4. B_ϕ (toroidal) and B_z (axial) in the layer are uniformly distributed zero-mean random variables normalized so that $\langle B_\phi^2 \rangle^{1/2} = \langle B_z^2 \rangle^{1/2}$.



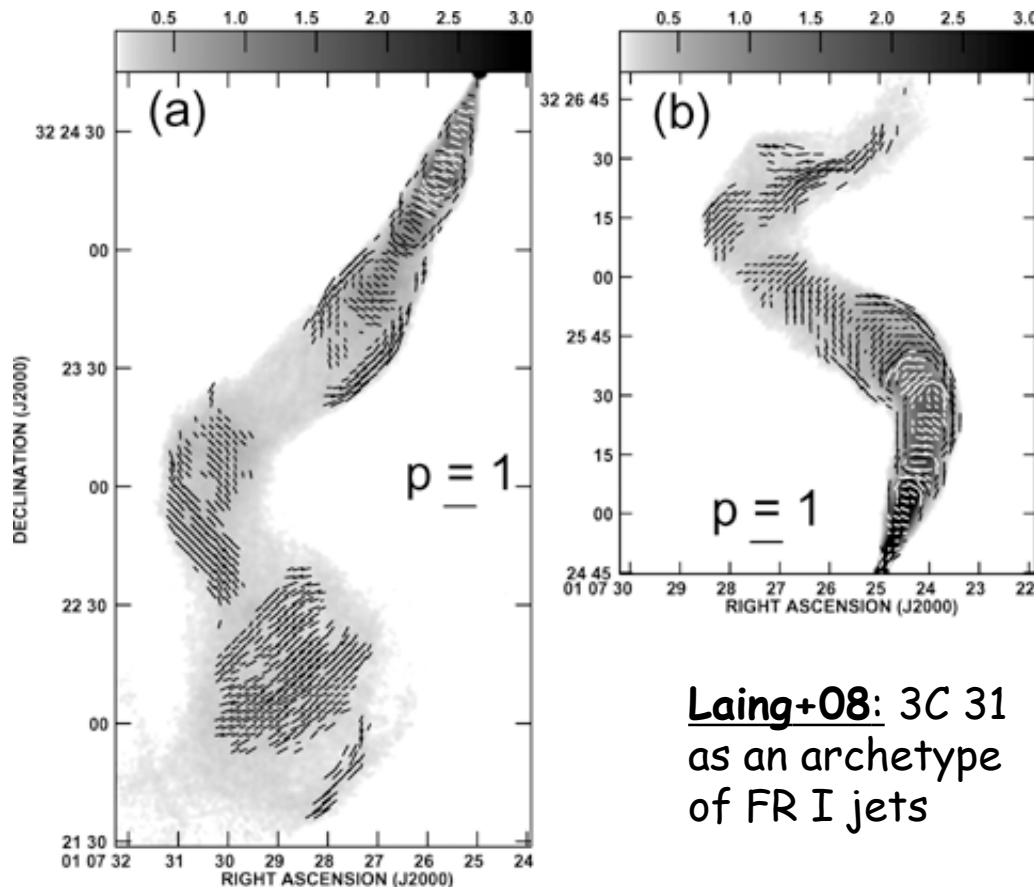
Data not consistent with globally ordered helical MF

Synchrotron Chandra Jets?



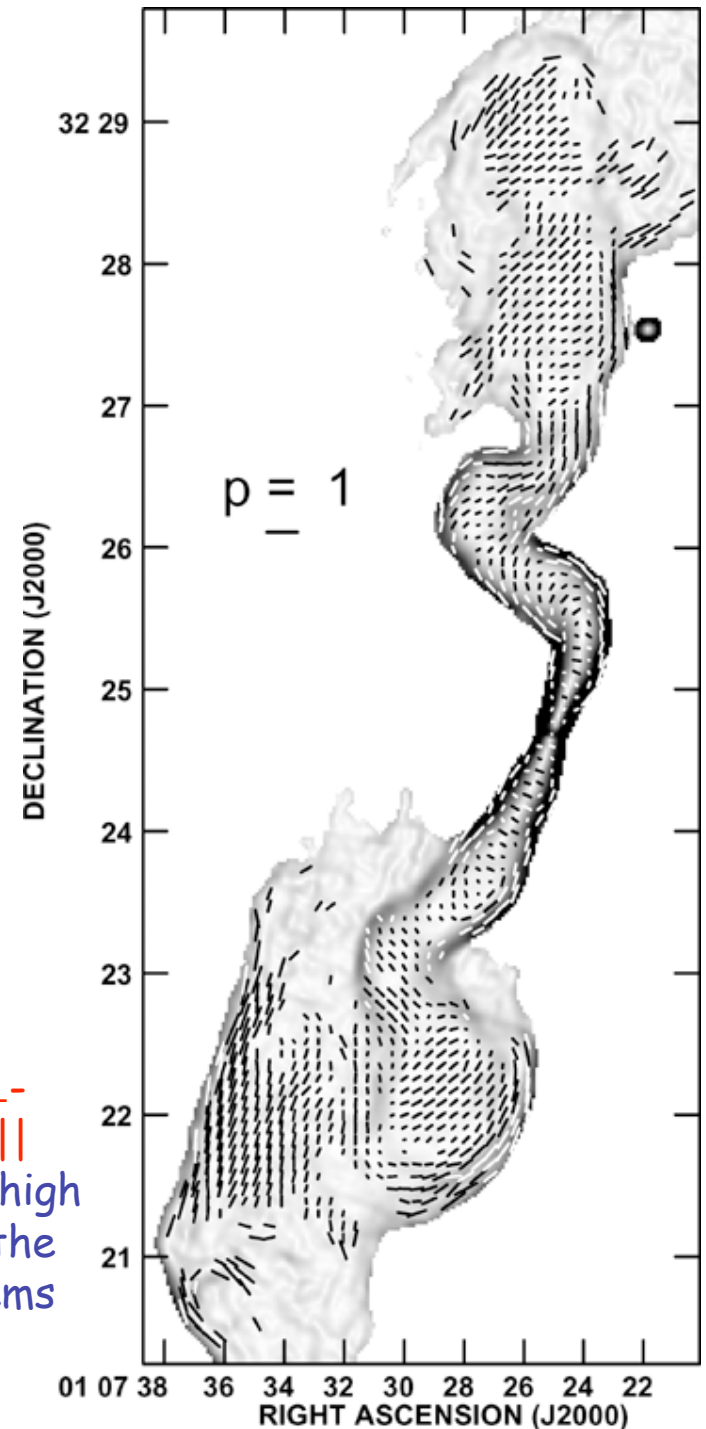
The spectral character of the broad-band emission of 3C 273 jet (Jester+ 07), as well as the detection of the X-ray counterjet in FR II radio galaxy 3C 353 (Kataoka+08), indicates that the synchrotron scenario for the X-ray emission of Chandra quasar jets may be more likely than the IC/CMB model. In such a case, the jet MF may be as well stronger than or equal to the equipartition value.

FR I Jets



Laing+08: 3C 31
as an archetype
of FR I jets

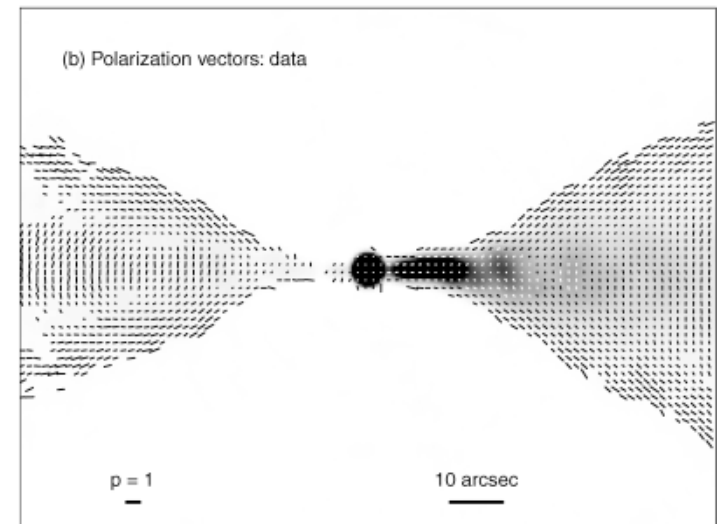
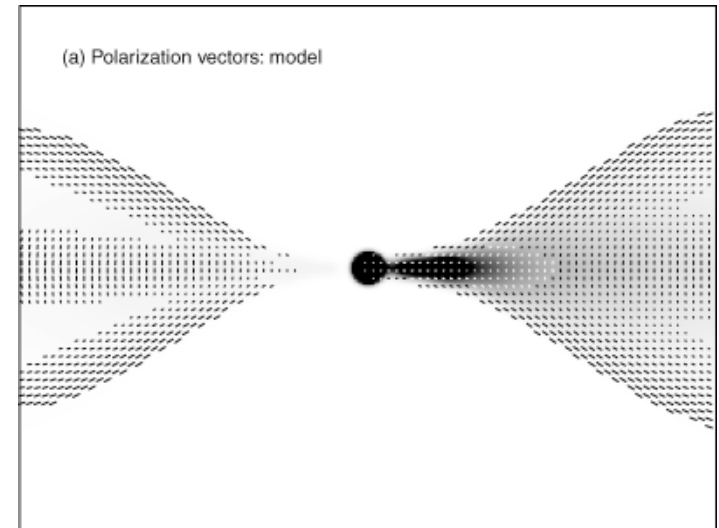
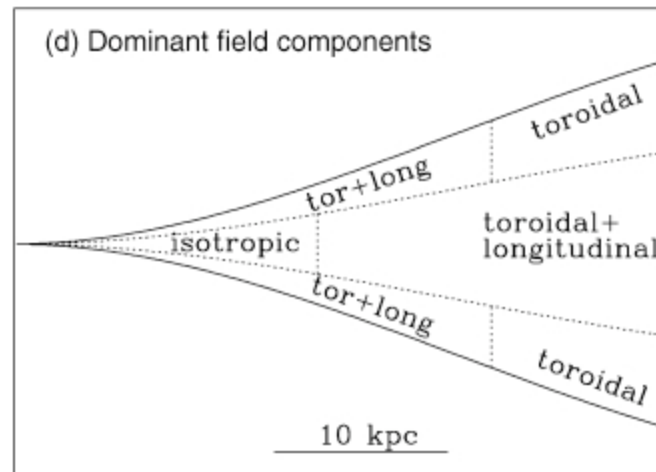
High linear polarization (50-60%) of 3C 31 jet. Initially B_{\perp} -spine/ B_{\parallel} -boundary layer morphology. Later altering B_{\perp} - B_{\parallel} configuration along the bending flow. Prominent arcs with high LP and aligned MF observed. Radio spectra are flatter at the edges of the jets, within the arcs, and where the flow seems to decelerate rapidly. The strongest synchrotron X-ray emission is not associated with the flattest radio spectra.



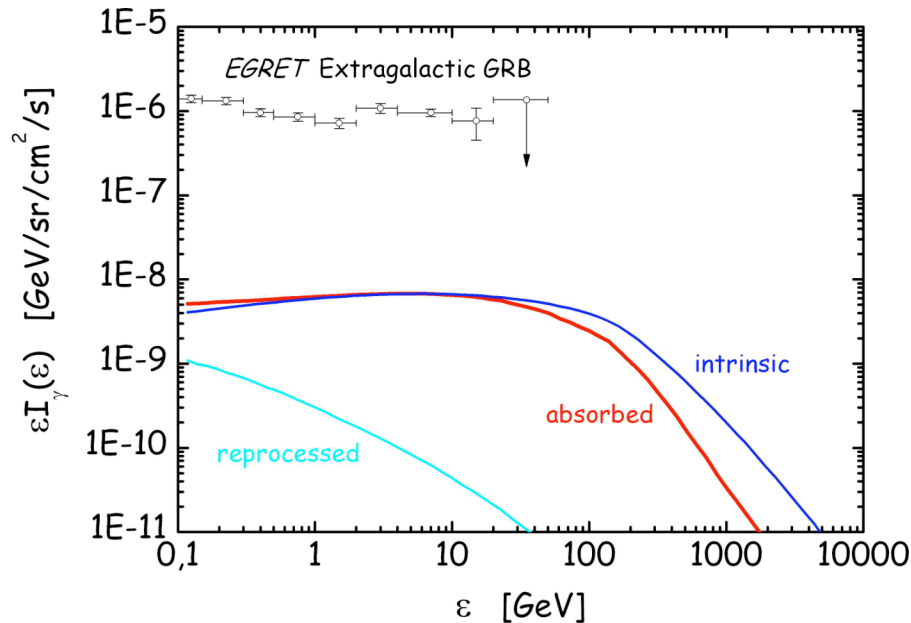
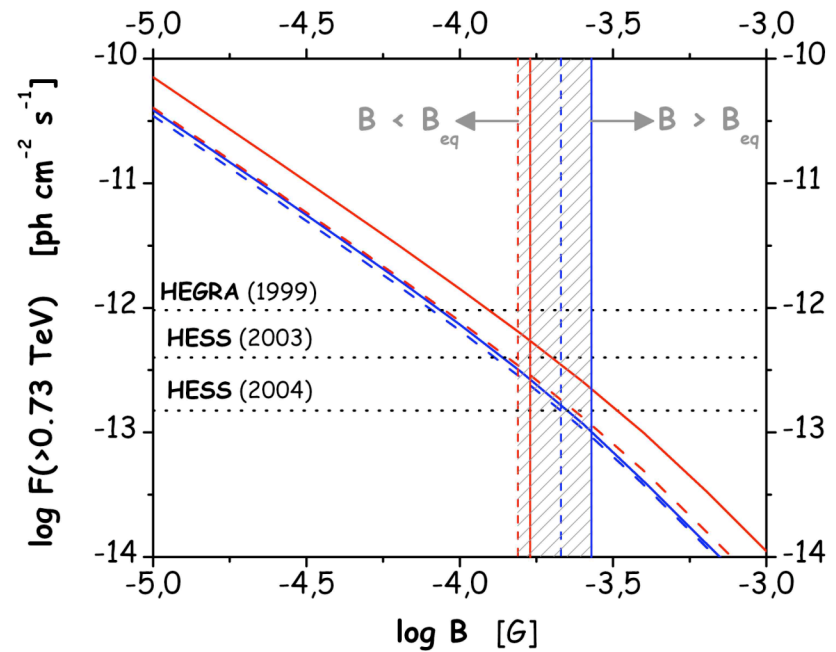
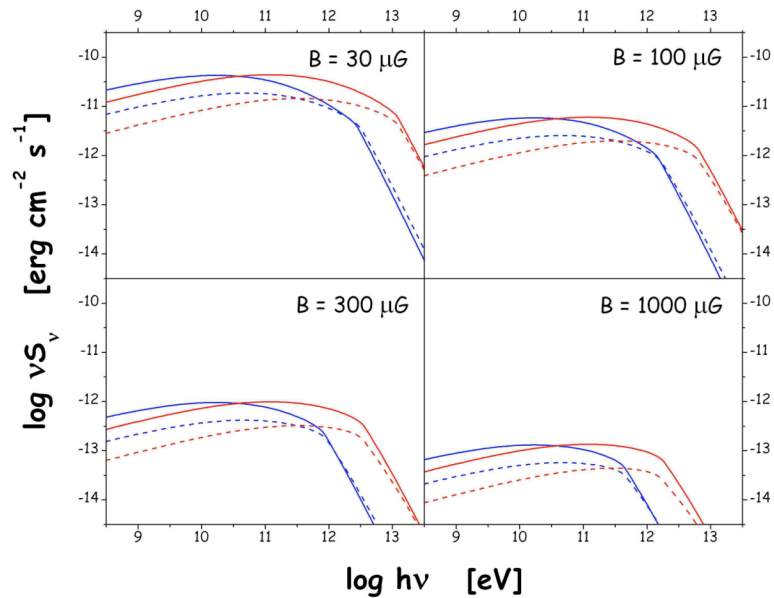
FR I Models

- **Laing & Bridle 02, 04** proposed “decelerating adiabatic” model for 3C 31 jet: radiating particles are accelerated before entering the region of interest and then lose energy only by the adiabatic losses, while the MF is frozen into and convected passively with the flow”.
- It was found that while the intensity distribution can be reproduced well in this model, the polarization data cannot be explained. The departures from adiabatic conditions in the 3C 31 jet suggest deviation from the flux-freezing condition and efficient in-situ particle acceleration (as required by the X-ray data).
- **Canvin & Laing 04, Canvin+05** relaxed the adiabatic condition, and provided good fits to several FR I jets (both intensity and polarization data).

MF is modelled as random on small scales but anisotropic. Globally ordered helical configuration is excluded.



How Strong Magnetic Field?



Stawarz+05: analysis of the expected TeV emission of kpc-scale jet in M87 radio galaxy, when compared with the HESS observations, indicate strong magnetic field $B \geq B_{eq}$.

Stawarz+06: similar analysis performed for the whole FR I population, compared with the extragalactic EGRET gamma-ray background, indicates $B > 0.1 B_{eq}$ on average in kpc-scale FR I jets.

GLAST will provide stronger constrains!

Large (>kpc) Scales - Summary

- Observational constraints seems to exclude globally ordered helical MF in large scale AGN jets.
- Magnetic confinement and strong (toroidal) magnetic field cannot be rejected on >kpc scales, although are not preferred by the data.
- More theoretical/numerical (3D) investigations on strongly magnetized jets is needed: a role of the magnetic reconnection (Romanova & Lovelace 92, Blackman 96, Lesh & Birk 98, Litvinenko+99, Larrabee+03), dynamo effect (De Young 80, Gvaramadze+88, Urpin 02), etc.
- Insufficient understanding of particle acceleration processes in (and, in general, microphysics of) relativistic plasma seems to be the main limiting factor in data interpretation.

Conclusions

- Magnetic field is crucial in launching AGN jets, since it mediates extraction of the energy and angular momentum from the black hole/accretion disk system.
- Magnetic field is crucial in formation of relativistic jets in AGNs, since it provides collimation and acceleration of nuclear outflows.
- A role of the magnetic field in AGN jets on large scales (confinement, stability, morphology) is still an open question.
- We do not know exactly how the jet magnetic field mediates energy dissipation (particle acceleration) processes, and therefore how it determines/shapes high-energy emission of extragalactic jets.